Available online at www.sciencedirect.com
SCIENCE DIRECT®
Journal of Human Evolution 48 (2005) 45–84

Evolution of the brainstem orofacial motor system in primates: a comparative study of trigeminal, facial, and hypoglossal nuclei

Chet C. Sherwood[a,b,*], Patrick R. Hof[b,c,d], Ralph L. Holloway[d,e], Katerina Semendeferi[f], Patrick J. Gannon[d,g], Heiko D. Frahm[h], Karl Zilles[h]

[a]*Department of Anthropology and School of Biomedical Sciences, Kent State University, Kent, OH 44242*
[b]*Foundation for Comparative and Conservation Biology, Hagerstown, MD 21740*
[c]*Department of Neuroscience, Mount Sinai School of Medicine, New York, NY 10029*
[d]*New York Consortium in Evolutionary Primatology, New York, NY*
[e]*Department of Anthropology, Columbia University, New York, NY 10025*
[f]*Department of Anthropology, University of California, San Diego, La Jolla, CA 92093*
[g]*Department of Otolaryngology, Mount Sinai School of Medicine, New York, NY 10029*
[h]*C. und O. Vogt Institut für Hirnforschung, Heinrich-Heine-Universität, Düsseldorf, Germany*

Received 5 May 2004; accepted 5 October 2004

Abstract

The trigeminal motor (Vmo), facial (VII), and hypoglossal (XII) nuclei of the brainstem comprise the final common output for neural control of most orofacial muscles. Hence, these cranial motor nuclei are involved in the production of adaptive behaviors such as feeding, facial expression, and vocalization. We measured the volume and Grey Level Index (GLI) of Vmo, VII, and XII in 47 species of primates and examined these nuclei for scaling patterns and phylogenetic specializations. Allometric regression, using medulla volume as an independent variable, did not reveal a significant difference between strepsirrhines and haplorhines in the scaling of Vmo volume. In addition, correlation analysis using independent contrasts did not find a relationship between Vmo size or GLI and the percent of leaves in the diet. The scaling trajectory of VII volume, in contrast, differed significantly between suborders. Great ape and human VII volumes, furthermore, were significantly larger than predicted by the haplorhine regression. Enlargement of VII in these taxa may reflect increased differentiation of the facial muscles of expression and greater utilization of the visual channel in social communication. The independent contrasts of VII volume and GLI, however, were not correlated with social group size. To examine whether the human hypoglossal motor system is specialized to control the tongue for speech, we

* Corresponding author. Department of Anthropology, Kent State University, 226 Lowry Hall, Box 5190, Kent, OH 44242-0001. Tel.: +1 330 672 5121; fax: +1 330 672 2999.
E-mail address: csherwoo@kent.edu (C.C. Sherwood).

0047-2484/$ - see front matter
doi:10.1016/j.jhevol.2004.10.003

tested human XII volume and GLI for departures from nonhuman haplorhine prediction lines. Although human XII volumes were observed above the regression line, they did not exceed prediction intervals. Of note, orang-utan XII volumes had greater residuals than humans. Human XII GLI values also did not differ from allometric prediction. In sum, these findings indicate that the cranial orofacial motor nuclei evince a mosaic of phylogenetic specializations for innervation of the facial muscles of expression in the context of a generally conservative scaling relationship with respect to medulla size.

Keywords: Comparative neuroanatomy; Brain evolution; Communication; Facial expression; Vocalization; Speech; Language evolution; Muscles of mastication; Tongue

Introduction

The orofacial region is an anatomical point of intersection for respiratory, sensory, feeding, and communication behaviors. As such, natural selection has produced great variety in the structure and function of this region in response to diverse ecological and social pressures. Among primates, interspecific variation in the anatomy and kinematics of orofacial muscles underlies diversified specializations in functions such as mastication, vocalization, facial expression, and speech. Here we examine morphometric scaling patterns in the brainstem orofacial motor system of primates with the aim of further elucidating the neural substrates of phylogenetic differences in orofacial behaviors.

The production of communication signals relies on the coordinated actions of orofacial muscles. Repertoires of facial expressions and vocalizations vary among primate species in association with the combined influence of sensory ecology, phylogenetic history, social organization, and cognitive abilities (van Hooff, 1967; Chevalier-Skolnikoff, 1973; Preuschoft and van Hooff, 1995; Hauser, 1996). In this regard, prosimians primarily utilize olfactory cues in sociosexual signaling, whereas anthropoids rely more heavily on visual displays, such as facial expression, in mediating social interactions (van Hooff, 1962; Schultz, 1969; Peters and Ploog, 1973; Zeller, 1987). In stem anthropoids, the elaboration of facial expression may have coevolved with enhanced visual acuity in a diurnal niche involving more convergent and frontated orbits, loss of the tapetum lucidum, high cone density in the central retina, low degrees of retinal summation, a foveate macula, and magnified representation of the central visual field within the brain (Allman, 1999; Ross, 2000). These adaptations increase the sensitivity of the visual system to stimuli occupying a small portion of the central visual field, such as the face of social partners. Indeed, there is strong evidence that faces and facial expressions constitute a special class of stimuli in the higher-order visual system of anthropoids. Groups of neurons that are selectively activated when presented with pictures of faces and facial expressions have been found in the inferior temporal cortex (Desimone et al., 1984; Hasselmo et al., 1989), the cortex of the superior temporal sulcus (Bruce et al., 1981; Perrett et al., 1982; Hasselmo et al., 1989), and the amygdala (Rolls, 1984; Leonard and Rolls, 1985; Adolphs et al., 1995) of macaque monkeys. Neuroimaging studies in humans reveal homologous regions in the temporal cortex that are activated by these stimuli (Puce et al., 1996; Kanwisher et al., 1997). In this context, it is interesting that Preuss and Goldman-Rakic (1991) found more cytoarchitectural subdivisions of the superior temporal cortex in macaques as compared to galagos, possibly reflecting an anatomical correlate of visual specialization in anthropoids for the perception of faces. Among great apes and humans, facial expressions involve a high degree of mobility, are under voluntary control, and are thought to be capable of communicating nonemotional signals for the purpose of deception and amusement (van Lawick-Goodall, 1968; Chevalier-Skolnikoff, 1982; de Waal, 1982; Goodall, 1986; Byrne and Whiten, 1992).

The muscles of the orofacial region also contribute to the formation of the vocal tract. Movements

of articulating structures in the supralaryngeal vocal tract (SVT), namely the soft palate, jaws, tongue, and lips, are critical in filtering and modifying the waveform produced at the vocal cords. These orofacial movements effectively change the resonance characteristics of the SVT by altering its length and shape, thereby varying the spectral energy of the fundamental frequency (Hauser and Schon Ybarra, 1994). As with non-human primate vocalizations, in human speech the movements of SVT articulators must be precisely synchronized with the vibrations of the vocal cords to clearly differentiate contrasting phonemes. A tenth of a millisecond difference in the timing of vocal cord vibration onset relative to SVT movements can cause perceptible differentiation of phonetic elements (Fitch, 2000). With a specialized anatomical configuration of the SVT such as a descended larynx and expanded oropharyngeal space, the adult human vocal apparatus is capable of achieving a wider range of articulatory configurations than any other primate (Lieberman, 2002). In part, this is because the adult human tongue has evolved to become relatively thick, with a substantial portion of its root forming the anterior wall of the pharynx (Laitman et al., 1978; Lieberman, 1984). This morphologic arrangement enables the formation of a wide range of vowel sounds. Indeed, clinical patients with bilateral paralysis of the tongue have severely affected articulation of the consonants "t," "d," "td," as well as all vowel sounds (Kimura, 1993). Although the human SVT has clearly undergone structural reorganization in order to facilitate rapid spoken language, other data suggest that human speech also relies on conservative functional neuromotor substrates. Studies of humans and macaques, for example, suggest that tongue kinematics in human speech may not be significantly different from feeding-related movements (Hiiemae, 2000; Hiiemae et al., 2002). And MacNeilage (1998) has shown that the syllabic structure of speech utilizes mandibular oscillations that are reminiscent of non-speech motor patterns of other primates. More comparative data on the physiology of the orofacial motor system in humans and other primates are needed, however, to illuminate in what respects, if any, speech involves specialized movement patterns of SVT articulators.

Along with their role in communication systems, the orofacial muscles also subserve a critical function in feeding adaptations. Food preparation and ingestion primarily involve actions of the teeth and mandible effected by contraction of the muscles of mastication. Each species tends to concentrate on consuming a limited set of food items depending on its particular energy and nutrient requirements. Primates that feed on plant materials that are high in structural carbohydrates, such as leaves, bark, and pith, require specializations of the molar teeth, mandible, gut, and muscles of mastication (Martin, 1990). Experimental data from several anthropoid taxa indicate that mastication of tough foods involves the recruitment of greater balancing-side muscle force from the deep masseter (Hylander and Crompton, 1986; Hylander and Johnson, 1993, 1994; Hylander et al., 2000) as well as more daily chewing cycles and larger average bite force (Walker and Murray, 1975; Lucas et al., 2000). Several structural features of the masticatory apparatus of folivores have been hypothesized to be adaptations for processing a tougher diet. In particular, comparative evidence suggests that folivores exhibit larger masseter, medial pterygoid, and temporalis muscles compared to primates that consume more pliant foods (Turnbull, 1970; Herring and Herring, 1974; Ravosa, 1990; Taylor, 2002). Other data indicate that, rather than simply enlarging masticatory muscles, folivores achieve increased bite force on the postcanine tooth row by positioning the elements of the musculoskeletal chewing apparatus in such a way as to improve mechanical advantage (Herring and Herring, 1974; Hylander, 1979; Spencer, 1998).

Despite the wealth of information available regarding phylogenetic variation in adaptations of the orofacial region, there is a paucity of data concerning interspecific differences in the neural control of orofacial muscles. Four cranial nuclei of the brainstem provide motor innervation to the orofacial muscles (Fig. 1). Motoneurons of the trigeminal motor nucleus (Vmo) supply the muscles of mastication and a few muscles of the palate (i.e., tensor veli palatini) and upper neck (i.e., anterior belly of the digastric). The facial nucleus (VII) contains motoneurons that innervate the

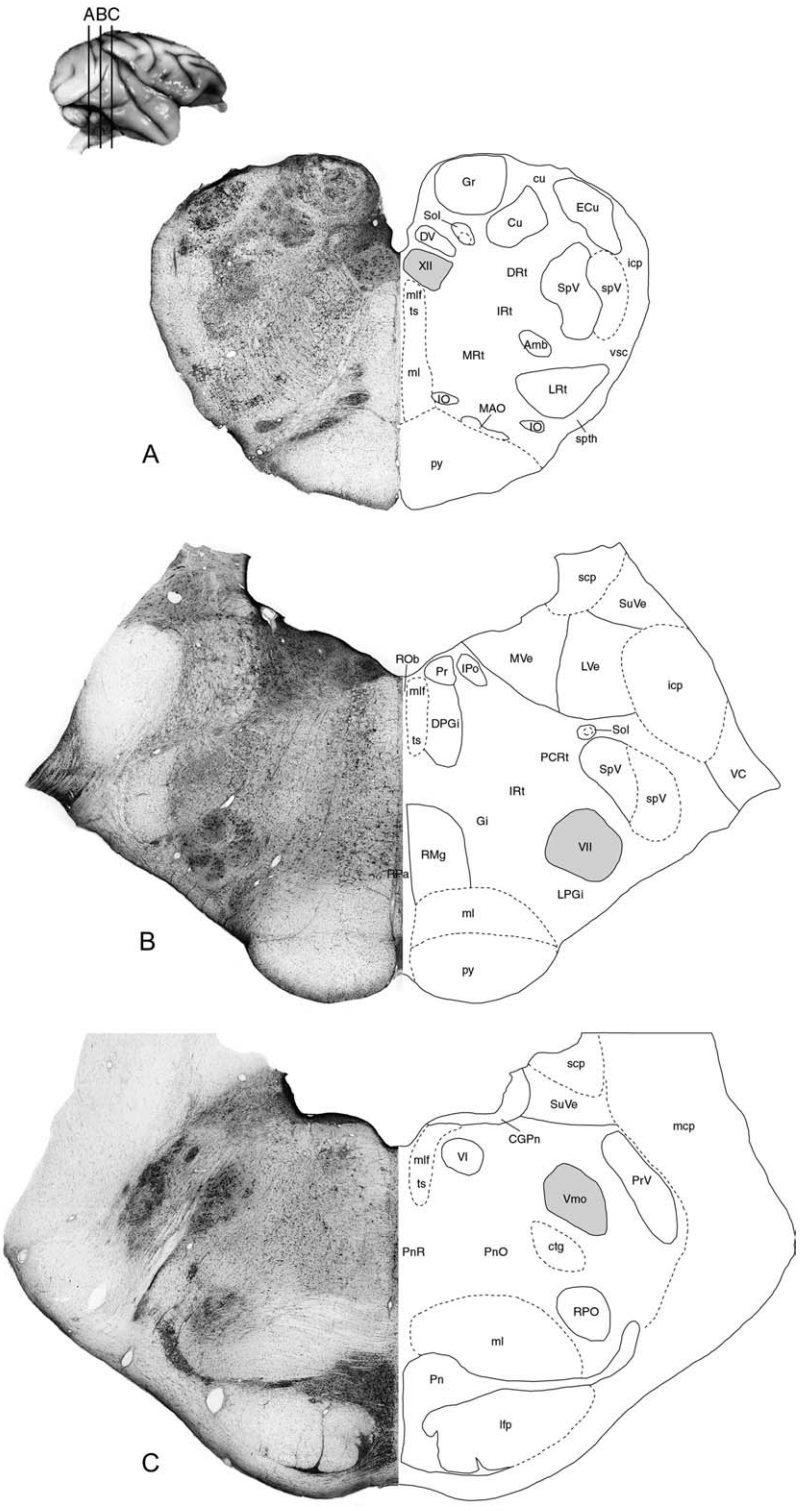
ABC
A
Gr
cu
ECu
Sol
Cu
DV
XII
DRt
icp
SpV
spV
mlf
ts
IRt
Amb
vsc
MRt
ml
LRt
IO
MAO
IO
spth
py
B
scp
SuVe
ROb
Pr
IPo
MVe
LVe
icp
mlf
DPGi
Sol
ts
PCRt
SpV
VC
IRt
spV
Gi
VII
RMg
LPGi
ml
py
C
scp
SuVe
mcp
CGPn
mlf
VI
ts
PrV
Vmo
PnR
PnO
ctg
RPO
ml
Pn
lfp

superficial facial muscles, including the "muscles of facial expression," the muscles of the rhinarium and pinnae, as well as the posterior belly of the digastric muscle in the upper neck. Motoneurons of the hypoglossal nucleus (XII) supply all the intrinsic and all but one of the extrinsic (i.e., palatoglossus) muscles of the tongue. And nucleus ambiguus motoneurons innervate muscles of the pharynx, larynx, and esophagus. Although the brainstem is considered to be the brain's most plesiomorphic component (Stephan et al., 1970; Finlay and Darlington, 1995), comparative studies of mammals have shown that the anatomy of brainstem nuclei may reflect ecological adaptations and specializations of peripheral structures (Matano, 1986; Baron et al., 1988, 1990, 1996; Glendenning and Masterton, 1998; Hutcheon et al., 2002). For example, semiaquatic insectivores have a relatively large sensory trigeminal complex in connection with abundant and elongated mystacial vibrissae used in teletactile functions (Baron et al., 1990), nectar feeding glossophagine bats with long protrusile tongues have relatively enlarged XII (Baron et al., 1996), and the relative volume of brainstem auditory nuclei (i.e., cochlear nuclei and the superior olivary complex) is larger in insectivorous bats compared to phytophages (Hutcheon et al., 2002). Thus, it is possible that the evolution of specialized orofacial behaviors in primates has been accompanied by reorganization of brainstem cranial motor nuclei.

Along these lines, paleoanthropologists have recently debated the usefulness of hypoglossal canal size as an indicator of the onset of speech abilities in hominin paleospecies (Kay et al., 1998; DeGusta et al., 1999; Jungers et al., 2003). The hypoglossal canal is a basioccipital foramen that transmits the hypoglossal nerve. Although researchers now agree that hypoglossal canal size cannot be used as a reliable index of speech abilities due to high levels of intraspecific variability (DeGusta et al., 1999; Jungers et al., 2003), the underlying premise that the hypoglossal nerve provides more dense innervation to the human tongue compared to other primates has remained unchallenged and untested. Indeed, notwithstanding the absence of comparative data on the hypoglossal motor system in primates, it has become accepted by some authors that the human tongue must receive relatively dense innervation and be more mobile to meet the kinematic demands of speech (e.g., Fitch, 2000; Nishimura et al., 2003).

As part of our ongoing investigation of the comparative neuroanatomy of the orofacial motor system in primates (Sherwood et al., 2003, 2004a,b), this study presents an analysis of morphometric scaling and specializations of cranial nerve orofacial motor nuclei. In particular, this study examines whether (1) departures from volumetric and cytoarchitectural scaling of orofacial motor nuclei are associated with the evolution of particular phylogenetic groups such as haplorhines, hominids (sensu Gray, 1825 – including great apes and humans), or humans, and (2) whether interspecific variation in the organization of orofacial motor nuclei is related to particular socioecological adaptations.

Fig. 1. Nissl-stained coronal sections through the brainstem of *Macaca fascicularis* showing the location of orofacial motor nuclei. Abbreviations: Amb, Nucleus ambiguus; CGPn, Central gray of the pons; ctg, Central tegmental tract; Cu, Cuneate nucleus; cu, Cuneate fasciculus; DPGi, Dorsal paragigantocellular nucleus; DRt, Dorsal reticular nucleus; DV, Dorsal motor nucleus of vagus; ECu, External cuneate nucleus; Gi, Gigantocellular reticular nucleus; Gr, Gracile nucleus; icp, Inferior cerebellar peduncle; IO, Inferior olive; IPo, Interpositus nucleus; IRt, Intermediate reticular nucleus; lfp, Longitudinal fasciculus of the pons; LPGi, Lateral paragigantocellular nucleus; LRt, Lateral reticular nucleus; LVe, Lateral vestibular nucleus, MAO, Medial accessory olive; mcp, Middle cerebellar peduncle; ml, Medial lemniscus; mlf, medial longitudinal fasciculus; MRt, Medial reticular nucleus; MVe, Medial vestibular nucleus; PCRt, Parvicellular reticular nucleus; Pn, Pontine nuclei; PnO, Pontine reticular nucleus, oral part; PnR, Pontine raphe nucleus; Pr, Prepositus nucleus; PrV, Principal sensory trigeminal nucleus; py, Pyramidal tract; RMg, Raphe magnus nucleus; ROb, Raphe obscurus nucleus; RPa, Raphe pallidus nucleus; RPO, rostral periolivary region; scp, Superior cerebellar peduncle; Sol, Solitary nucleus and tract; spth, Spinothalamic tract; spV, Spinal trigeminal tract; SpV, spinal trigeminal nucleus; SuVe, Superior vestibular nucleus; ts, Tectospinal tract; VC, Ventral cochlear nucleus; VII, facial nucleus; VI, abducens nucleus; Vmo, trigeminal motor nucleus; vsc, Ventral spinocerebellar tract; XII, hypoglossal nucleus.

Materials and methods

Specimens and tissue preparation

Data were collected from Vmo, VII, and XII of 102 individuals, representing 47 species of primates from every subfamily of the order (Table 1). Although the structure of the nucleus ambiguus is relevant to the orofacial motor adaptations of primates, it is not practical to include in morphometric analyses because it consists of a narrow discontinuous column of scattered neurons (Ariëns Kappers et al., 1936; Crosby et al., 1962), making it difficult to quantify reliably (Stephan et al., 1991). The sample used in this study derived from comparative neuroanatomical slide collections of coronally sectioned brains located at the C. & O. Vogt-Institut für Hirnforschung, Universität Düsseldorf. Most of the specimens have been included in previous reports by Stephan and colleagues, and details of specimen preparation methodology can be found therein (Stephan et al., 1970, 1981, 1988). Briefly, brain specimens were fixed with either Bouin's fluid or 10% formalin, embedded in paraffin, sectioned between 10 and 25 μm, and a series of equidistant sections was stained for Nissl substance with cresyl violet. Considering the relatively poor representation of hominoids in Stephan's collection and the relevance of these species to assessments of human neural specializations, additional specimens prepared by one of the authors (K.Z.) and his coworkers at Düsseldorf were included in this study to provide improved interspecific and intraspecific sampling of these taxa. Importantly, data were collected from *Pongo pygmaeus* and *Pan paniscus* specimens that were not included in the original Stephan et al. (1981) dataset. These additional specimens were fixed by immersion in either 4% formalin or Bodian's solution, embedded in paraffin, sectioned with a microtome at 20 μm, and an equidistant series of sections was stained for Nissl substance with a modification of the Gallyas silver impregnation technique for cell bodies (Gallyas, 1971; Merker, 1983). Brain weight was recorded for all individuals prior to histological preparation, thereby allowing subsequent calculation of shrinkage correction factors for all volumetric measurements.

Image acquisition

Every available section containing the left Vmo, VII, and XII was digitally photographed for each specimen (Fig. 2). Only one side was analyzed because previous studies have shown that cranial nerve motor nuclei do not exhibit morphometric asymmetries (Nara et al., 1989, 1991). Digital micrographs were obtained using an Olympus BH-2 microscope with a PlanApo 4× objective and a Nikon CoolPix 995 digital camera (3.4 Megapixel CCD). For each nucleus, the optical zoom on the digital camera was adjusted to fit the nucleus into the field of view. Using a consistent magnification factor throughout, digital photomicrographs of every section containing the nucleus were collected, along with a micrometer scale for metric calibration. Final image resolution ranged from 0.6 to 1.7 pixels per μm, depending on the size of the nucleus.

Measurement of nucleus volume

The planimetric volume of each nucleus was measured from digital image stacks opened in ImageJ software version 1.26t (http://rsb.info.nih.gov/ij/). All consecutive equidistant sections that were available through each nucleus were measured. The section sampling interval was variable, depending upon the overall size of the brain (range = 1:4 to 1:40). On average, 6.5 ± 2.1 (mean $\pm$ SD) sections were measured for Vmo, 7.6 ± 2.5 sections for VII, and 10.3 ± 2.8 sections for XII. After calibrating the software to the micrometer scale contained in the image stack directory, contours were drawn around the nucleus as it appeared in each coronal section using the freehand drawing tool in the software and the surface area bounded by the contour was calculated. Total nucleus volume (V_N) was obtained according to the Cavalieri principle by multiplying the sum of the surface areas in each section ($\sum A_S$) by section thickness (T_S) and the interval distance between sections (D_S) using the equation $V_N = \sum A_S \times T_S \times D_S$. Reliability of volumetric measurements was evaluated by repeating measurements of VII in five randomly selected specimens. Measurement error, calculated as the mean

Table 1
Species means and standard deviations for volumes of medulla and orofacial motor nuclei (left side only) (mm^3)

Species	N	Medulla volume		Vmo volume		VII volume		XII volume	
		Mean	SD	Mean	SD	Mean	SD	Mean	SD
Microcebus murinus	6	99.03	12.49	0.13	0.02	0.29	0.06	0.25	0.03
Cheirogaleus major	2	381.62	17.17	0.52	0.12	0.78	0.01	0.92	0.28
Cheirogaleus medius	2	202.38	5.62	0.30	0.06	0.52	0.01	0.57	0.06
Eulemur fulvus	3	909.39	93.37	1.04	0.20	1.39	0.15	1.52	0.26
Varecia variegata	1	1420.00	-	1.61	-	2.65	-	3.13	-
Lepilemur ruficaudatus	3	449.28	48.21	0.69	0.09	0.91	0.08	1.15	0.23
Avahi laniger laniger	2	553.35	27.87	0.88	0.12	1.07	0.08	0.74	0.03
Avahi laniger occidentalis	2	508.46	57.67	0.82	0.06	0.81	0.00	0.62	0.01
Propithecus verreauxi	2	1222.63	32.91	1.68	0.32	1.96	0.01	1.62	0.13
Indri indri	2	1342.01	47.53	1.72	0.21	2.45	0.30	1.84	0.18
Daubentonia madagascariensis	1	1517.10	-	1.91	-	2.00	-	2.19	-
Loris tardigradus	2	287.23	77.13	0.53	0.14	0.56	0.10	0.47	0.02
Nycticebus coucang	2	528.14	27.69	1.04	0.27	0.95	0.12	0.76	0.21
Perodicticus potto	2	679.74	8.71	1.11	0.22	1.29	0.31	1.28	0.19
Galago senegalensis	1	254.30	-	0.29	-	0.59	-	0.35	-
Otolemur crassicaudatus	2	539.87	89.56	0.87	0.05	1.41	0.19	0.81	0.26
Galagoides demidoff	2	169.13	14.08	0.22	0.02	0.48	0.01	0.28	0.04
Tarsius syrichta	2	206.85	32.59	0.36	0.05	0.75	0.18	0.28	0.08
Callithrix jacchus	4	318.24	39.74	0.47	0.07	0.54	0.10	0.44	0.04
Cebuella pygmaea	2	185.00	10.47	0.28	0.07	0.27	0.00	0.28	0.05
Saguinus midas	2	428.47	8.48	0.52	0.02	0.63	0.03	0.56	0.04
Saguinus oedipus	3	413.31	64.68	0.54	0.09	0.50	0.10	0.62	0.07
Callimico goeldii	1	460.10	-	0.55	-	0.48	-	0.54	-
Cebus albifrons	2	1738.26	78.27	2.16	0.13	2.47	0.55	1.98	0.25
Aotus trivirgatus	4	675.30	54.99	0.86	0.12	1.24	0.34	0.87	0.13
Callicebus moloch	2	786.82	71.55	1.00	0.14	1.18	0.13	0.98	0.01
Saimiri sciureus	1	721.53	-	0.76	-	0.84	-	0.82	-
Pithecia monachus	2	1008.88	24.08	1.32	0.18	1.34	0.10	1.36	0.19
Alouatta seniculus	2	1593.25	400.50	2.26	0.58	1.73	0.62	1.62	0.42
Ateles geoffroyi	1	1833.67	-	1.80	-	1.65	-	1.78	-
Lagothrix lagothricha	3	2109.54	323.24	2.56	0.47	2.68	0.34	2.13	0.34
Macaca mulatta	2	2329.14	126.13	3.84	0.58	4.92	0.61	3.85	0.57
Lophocebus albigena	1	2670.59	-	3.27	-	4.31	-	3.06	-
Papio anubis	1	5171.17	-	6.16	-	7.44	-	4.62	-
Cercopithecus ascanius	2	1802.09	240.43	2.07	0.27	2.64	0.34	1.99	0.31
Cercopithecus mitis	1	1998.90	-	2.14	-	3.07	-	2.07	-
Miopithecus talapoin	2	1034.79	188.62	1.47	0.05	1.86	0.57	1.22	0.03
Erythrocebus patas	2	2615.67	112.28	2.33	0.30	4.59	0.19	2.40	0.29
Procolobus badius	2	2007.11	48.95	2.23	0.05	2.26	0.30	1.51	0.02
Pygathrix nemaeus	1	2206.11	-	2.18	-	2.79	-	1.57	-
Nasalis larvatus	1	2945.18	-	2.82	-	4.41	-	2.18	-
Hylobates lar	3	2249.16	118.66	1.96	0.08	2.06	0.24	2.44	0.30
Pongo pygmaeus	3	5172.05	579.77	6.31	2.54	12.82	5.70	12.11	2.26
Gorilla gorilla	3	8393.91	1385.35	9.49	1.89	13.26	3.60	10.20	2.79
Pan troglodytes	3	6027.39	1282.37	5.09	1.14	12.32	1.18	7.84	3.08
Pan paniscus	2	4152.02	710.28	2.89	0.12	7.50	0.96	4.09	1.21
Homo sapiens	5	9699.79	711.33	7.74	2.03	12.95	2.72	14.39	2.99

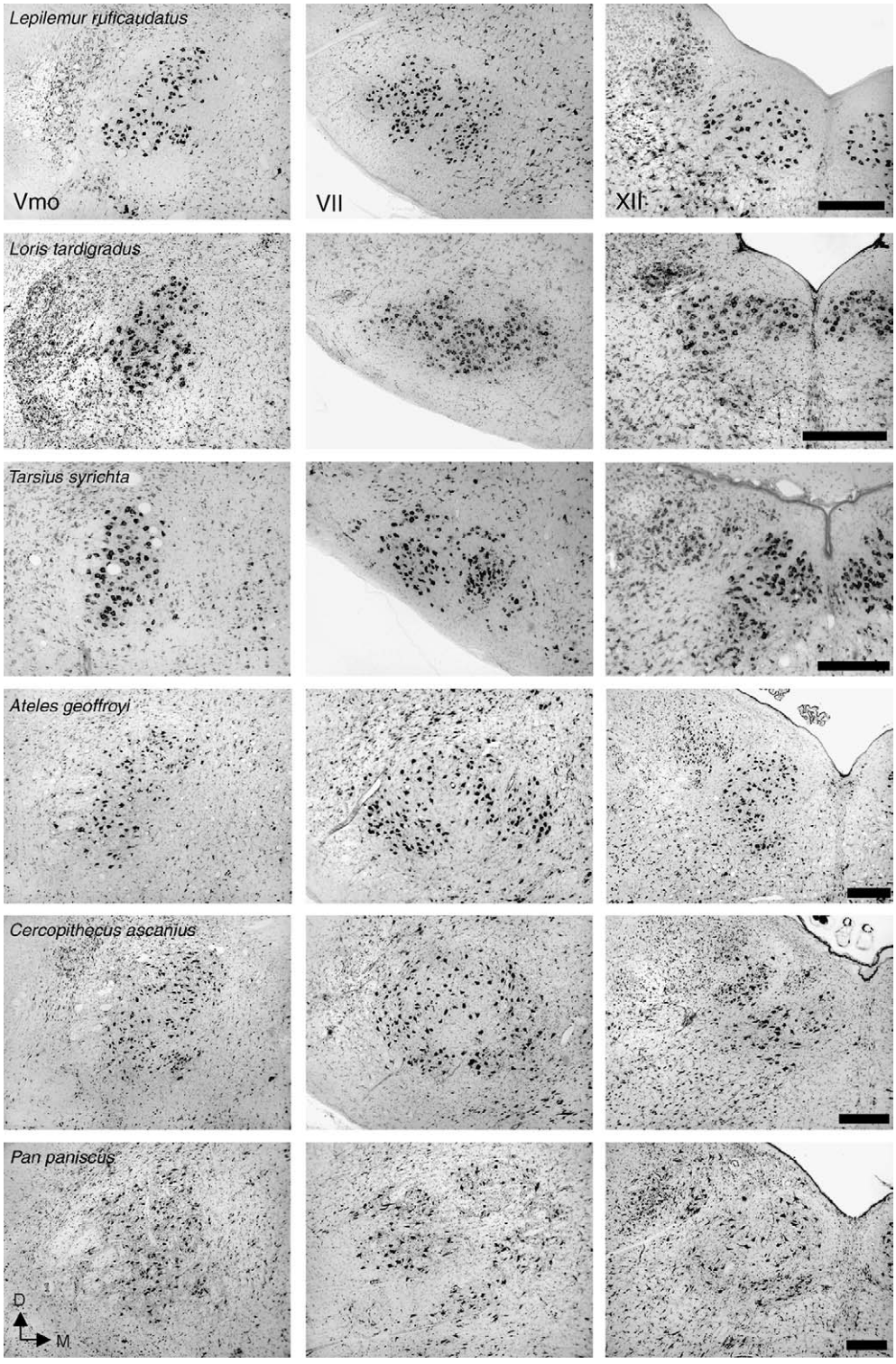
Lepilemur ruficaudatus
Vmo
VII
XII
Loris tardigradus
Tarsius syrichta
Ateles geoffroyi
Cercopithecus ascanius
Pan paniscus
D
M

of percent differences between repeated measurements, was 1.40% ± 0.92%.

Measurement of Grey Level Index

Volumetric measurements of brain structures provide an important initial estimate of processing capacity within a neural system. However, more subtle differences in the arrangement of cell types and their interconnections may also contribute significantly to interspecific differences in behavioral output. In consideration of this, the Grey Level Index (GLI) was measured for each nucleus. The GLI value is the proportion of an area of reference that is occupied by the projected profiles of all stained elements and provides an estimate of the fraction of tissue that contains neuronal somata, glial cell nuclei, and endothelial nuclei versus neuropil (Wree et al., 1982; Schleicher and Zilles, 1990). Since neuropil is occupied predominantly by dendritic processes, axons, and synapses, the GLI provides an indirect measure of the space available for interconnections (Wree et al., 1982; Schlaug et al., 1993; Pannese, 1994). The GLI method was employed because it can be performed with archival Nissl-stained slides, permitting the acquisition of quantitative cytoarchitectural data in a large and diverse sample of species. Furthermore, GLI values are minimally affected by interindividual variation in tissue shrinkage due to histological processing because the method calculates a relative measure of cellular profiles per unit area.

There is a non-linear increase in GLI with increasing section thickness. The inflection point of the exponential function that describes the relationship between GLI and section thickness occurs around 15 μm and reaches asymptote (Wree et al., 1982). Therefore, only specimens that were sectioned between 15 and 20 μm were measured for GLI. On this basis, several specimens used in volumetric analyses could not be included. GLI was measured from two adjacent sections located at the midbody of each nucleus. Prior to GLI measurement, images were processed in ImageJ software with background subtraction using a rolling ball algorithm (Sternberger, 1983), converted to binary by an automated threshold routine based on Rider and Calvard (1978), and dilation and erosion were applied to fill small holes representing light staining of cellular nuclei. Hole-filling was necessary to prevent artificially low GLIs in specimens stained for Nissl substance with cresyl violet compared to silver impregnation. The Gallyas silver stain results in dark labeling throughout the soma of large motoneurons, whereas cresyl violet staining results in dark labeling of the cytoplasm and pale staining within the cell nucleus. Measuring frames of 150 × 150 pixels were placed within the boundaries of the nucleus on the processed image to cover 50% of surface area and the total number of black pixels found within these frames was counted (Fig. 3). The GLI was calculated as the fraction of the measuring frame area (a total of 22,500 pixels) occupied by black pixels. The GLI value for a nucleus represents the mean of GLI measurements from all measuring frames.

Measurement of medulla volume

The volume of the medulla oblongata was used as the independent variable in allometric analyses. The medulla was chosen because it is the brain subdivision most proximal to the orofacial motor nuclei in anatomical location and a large number of afferent inputs to these nuclei derive from premotor neurons in the lateral medullary reticular formation. These premotor afferents supply multiple nuclei via axon collaterals and serve as an anatomical substrate for the integration of orofacial motor output in activities such as swallowing, mastication, respiration, vocalization, and facial expression (Li et al., 1993a,b and 1997; Fay and Norgren, 1997; Dauvergne et al., 2001; Popratiloff et al., 2001). Although body weight was available for most individuals, it was not used as an independent variable because it is susceptible to

Fig. 2. Nissl-stained coronal sections at high magnification showing Vmo, VII, and XII of various species. Scale bar = 400 μm. D = dorsal. M = medial.

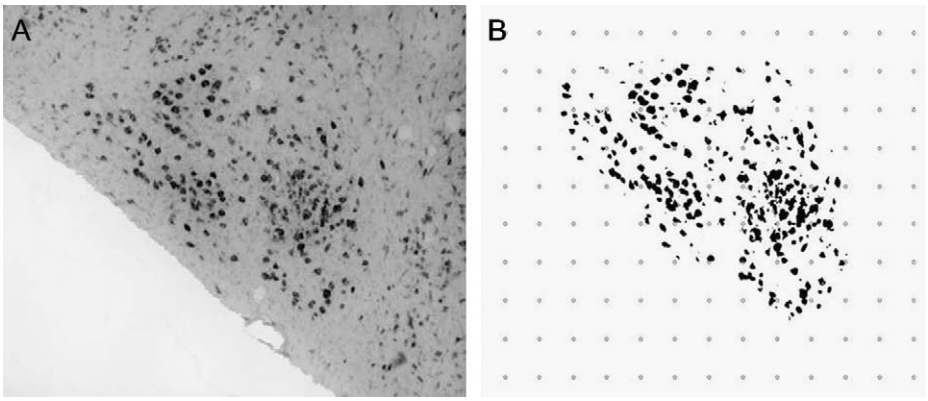

Fig. 3. GLI image conversion method. A Nissl-stained section of VII in *Tarsius syrichta* is shown (a). After background subtraction and conversion to binary, systematic randomly distributed measuring frames of 150 × 150 pixels are placed (b). GLI is measured within the measuring frames covering 50% of the total nucleus area.

various confounding factors, including health status, seasonal fluctuations, age, gravidity in females, and captivity (Stephan et al., 1988; Harvey and Krebs, 1990).

Medulla volumes of many specimens in the Stephan collection have been measured and reported previously (Stephan et al., 1970, 1981, 1988). For consistency, identical anatomical boundaries were used for measurement of medulla volumes in the additional specimens included in this study. For each specimen, at least 20 equidistant sections through the medulla were digitized with a CCD camera. Volumes were measured from calibrated digital image stacks in ImageJ using the Cavalieri principle as described above for the orofacial motor nuclei.

Data transformations

Volumes of brainstem nuclei and medulla were corrected for tissue shrinkage and standardized to species-typical brain volume following the method of Stephan et al. (1981). Individual shrinkage correction factors for each brain were obtained from H.D. Frahm (unpublished data) and MacLeod (2000). Species mean brain volumes used for standardization came from Stephan et al. (1981), except in the case of *Pongo pygmaeus* and *Pan paniscus*, which were not available in the original dataset. A species mean brain volume of 321.4 cm^3 was used for *Pongo pygmaeus* (Zilles and Rehkämper, 1988) and 311.2 cm^3 was used for *Pan paniscus* (Rilling and Insel, 1999).

It should be noted that, for several cases, the species mean medulla volumes reported here differ from those included in the original Stephan et al. (1981) dataset. These include: *Loris tardigradus*, *Cebuella pygmaea*, *Aotus trivirgatus*, *Macaca mulatta*, *Lophocebus albigena*, *Papio anubis*, *Cercopithecus ascanius*, *Hylobates lar*, *Gorilla gorilla*, *Pan troglodytes*, and *Homo sapiens*. These discrepancies can mostly be attributed to increased sample sizes (e.g., *Loris tardigradus*, *Macaca mulatta*, *Cercopithecus ascanius*, *Hylobates lar*, *Gorilla gorilla*, *Pan troglodytes*, and *Homo sapiens*). However, several specimens that were included in the Stephan et al. (1981) dataset are no longer available due to loss or damage. Therefore, to obtain correlated measurements of orofacial motor nuclei and medulla derived from the same individuals, intraspecific samples were either reduced (e.g., *Aotus trivirgatus* and *Papio anubis*) or substituted with other available specimens in which medulla volume was measured for this study (e.g., *Cebuella pygmaea* and *Lophocebus albigena*).

Statistical analysis

Nucleus volumes were analyzed for allometric scaling relationships by fitting lines to bivariate plots against medulla volume. The scaling of GLI

was calculated by regressing GLI against the cube root of nucleus volume. The cube root was taken to bring the bivariate data into the same dimensionality. Prior to fitting regressions, data were explored to determine whether raw values or logarithmic transformation would be more appropriate to fulfill assumptions of normality and homoscedasticity. In all cases, visual inspection of the plot of residuals versus observed values showed that the magnitude of residual variance tended to increase with larger structure size for the raw data. However, the residual variance distribution was not correlated with the observed value after logarithmic (base 10) transformation. Therefore, all regression analyses were carried out on log-transformed data.

Many of the analyses in this study involve regressing volumes of orofacial motor nuclei against medulla volume. Concern has been raised regarding the confounding effect of autocorrelation when a part is regressed against the whole from which it is derived (Deacon, 1990). In our analyses, however, the dependent variable (each orofacial motor nucleus) constituted less than 0.5% of the independent variable (total medulla), giving no reason to suspect that autocorrelation artificially inflates the fit of the regression or reduces sensitivity to allometric departures. Therefore, the volume of orofacial motor nuclei was not subtracted from medulla volume in allometric analyses.

Line-fitting was used to assess the scaling pattern of orofacial motor nuclei with respect to medulla volume and examine allometric departures from volumetric and GLI scaling as potential cases of adaptive specializations. If the correlation between variables is high, different methods of line-fitting, i.e., least squares (LS) and reduced major axis (RMA), yield similar results. Considering the very high correlations between nucleus volume and medulla volume in this study, scaling exponents differed very little between LS and RMA (see Results). Although both statistics are presented, the LS line was used to examine allometric departures because it produces residuals that are uncorrelated with the independent variable (Harvey and Krebs, 1990). Residuals from the LS line, thus, represent the degree to which changes in the dependent variable deviate from simple correlated responses of changes in the independent variable.

Phylogenetic methods

Species values cannot be treated as strictly independent data points in statistical analyses because close phylogenetic relatives will tend to be similar to one another due to shared common ancestry (Felsenstein, 1985; Harvey and Krebs, 1990; Harvey and Pagel, 1991; Purvis and Rambaut, 1995; Purvis and Webster, 1999). To overcome the problem of nonindependence in comparative data, the method of phylogenetically independent contrasts (IC) computes pairwise standardized contrast scores that represent independent character evolution that has occurred since the common ancestor of sister lineages (Felsenstein, 1985; Garland et al., 1992). These contrasts can then be subjected to conventional statistical analyses. Independent contrasts were calculated using the PDAP:PDTREE module of Mesquite software version 1.01 (Garland et al., 1999; Garland and Ives, 2000). In brief, ICs are calculated as the difference between the values of a trait in two sister taxa divided by the square root of the sum of their branch lengths. Branch lengths are assumed to be proportional to the accumulated variance in a trait over time based on a Brownian motion model of evolutionary change (Felsenstein, 1985). Since it is expected that unstandardized ICs will increase as a function of branch length, to prevent these values from having undue leverage in regression and correlation analysis, each IC is standardized by dividing it by the square root of the sum of its branch lengths (Garland et al., 1992). Independent contrasts were calculated from log-transformed data based on Purvis' (1995) composite phylogeny of the primates. After standardization, ICs were uncorrelated with their standard deviations, indicating that the branch lengths meet the assumption of the method (Garland et al., 1992).

Prior to performing scaling analyses, we examined the amount of phylogenetic signal in the dataset. Phylogenetic signal may be understood as the tendency for character states in closely related

species to resemble each other. To quantify the amount of phylogenetic signal in each trait, we calculated the descriptive statistic, K, following Blomberg et al. (2003). This method "indicates the strength of phylogenetic signal, as compared with an analytical expectation based solely on the tree structure (topology and branch lengths) and assuming Brownian motion character evolution" (Blomberg et al., 2003: p. 722). If $K = 1$, this implies that the trait displays precisely the amount of phylogenetic signal expected for Brownian motion evolution along the specified tree. If $K < 1$, then relatives are less similar than expected and, if $K > 1$, then relatives are more similar than expected. These analyses were carried out on the Purvis (1995) tree topology and branch lengths (untransformed) using the PHYSIG program provided by T. Garland, implemented in MATLAB version 6.5. Next, we examined the practical effect of phylogenetic bias in the data on scaling relationships. This was done by comparing IC regression slopes to the 95% confidence intervals of "nonphylogenetic" regressions based on species values. Overall, volumetric scaling coefficients were similar for phylogenetic and nonphylogenetic regressions (see Results), suggesting that the scaling relationships between these neuroanatomical variables are not excessively influenced by inherited similarity among close relatives. Therefore, we follow phylogenetic regression analyses with conventional nonphylogenetic approaches based on species values. Notwithstanding the statistical problems associated with allometric analysis of species values discussed above, this approach facilitates more ready comparison with previous studies and more intuitive interpretation of residuals.

To gain insight into possible adaptive associations of orofacial motor nucleus organization, correlations between neuroanatomical variables and socioecological variables were examined using ICs. Phylogenetic information is important in tests of hypotheses about correlated evolution between variables because closely related species will tend to share a cluster of traits due to common descent, potentially leading to spurious conclusions regarding the adaptive association between traits. In contrast, the finding of a significant correlation between traits based on ICs demonstrates that the variables have consistently covaried in a similar manner across multiple independent speciation events. We hypothesized that there may be a relationship between VII and sociality. It is possible that species with relatively more voluminous or interconnected VII are capable of performing finer movements of the facial muscles of expression to communicate subtle information among social partners. Data on social group size obtained from Barton (1999) were used as an index of the complexity of the social environment that an individual must negotiate (Dunbar, 1992, 1998). We also hypothesized that there may be a relationship between Vmo and diet because it has been suggested that folivores have relatively greater masticatory muscle mass. For this analysis, data on the percentage of leaves in the diet taken from Ross and Jones (1999) were used as an index of diet toughness.

All statistical analyses were performed using Statistica software version 6.0 (StatSoft, Inc., Tulsa, OK). Statistical significance was set at $\alpha = 0.05$ (two-tailed).

Results

Volumetric data—absolute size and percentage of medulla

Table 1 shows species means and sample sizes for volumetric measurements of Vmo, VII, XII and total medulla. Across primates, there is a 70-fold difference in volume between the largest and the smallest Vmo, a 45-fold difference for VII volume, and a 59-fold difference for XII volume. These values can be compared with the range of variation within primates for other brain components such as the medulla (97-fold), cerebellum (587-fold), and neocortex (1,360-fold).

Fig. 4 displays the distribution of nucleus volumes in primates and 30 species of insectivores taken from Stephan et al. (1991). The Insectivora are shown for comparison because they are the only other mammalian group from which extensive comparable data are available. In some older studies, "basal" insectivores were used to represent

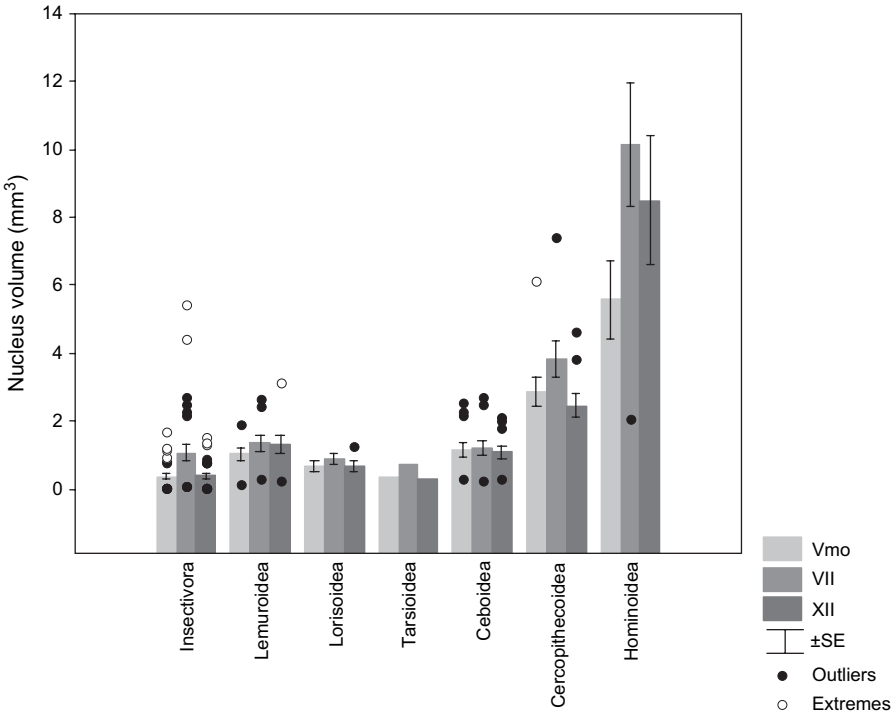

Fig. 4. Bar graph of the volume of each orofacial motor nucleus in insectivores and primates. Nucleus volumes represent data from one side only as indicated in Table 1.

a conservative eutherian grade of brain organization. Here, insectivore data are not intended to represent the ancestral eutherian condition, but rather are presented as another group of well-studied mammals that overlap with primates in medulla size. The total volume of the orofacial motor nuclei (i.e., Vmo + VII + XII) is generally similar across insectivores, lemuroids, lorisoids, tarsioids, and ceboids. However, the orofacial nuclei are substantially larger in cercopithecoids and hominoids. To examine the balance between the size of Vmo, VII, and XII, we used repeated-measures ANOVA with nucleus as a within factor and taxon as a between factor (i.e., Insectivora and primate superfamilies excluding tarsioids because of small sample size). There is a significant interaction effect of nucleus and taxon ($F_{10,140} = 14.22$, $p < 0.001$), indicating that there are phylogenetic differences in the relative sizes of orofacial nuclei with respect to one another. Post hoc tests revealed that, in most taxa, the orofacial motor nuclei are not significantly different in volume. However, in insectivores, VII is significantly larger than other nuclei (Bonferroni post hoc, both contrasts $p < 0.005$). In cercopithecoids, VII is significantly larger than XII (Bonferroni post hoc, $p < 0.001$). In hominoids, all orofacial motor nuclei differ significantly from one another in volume (Bonferroni post hoc, all contrasts $p < 0.005$).

Table 2 displays the size of each orofacial motor nucleus as a percentage of total medulla volume. The total volume of orofacial motor nuclei comprises a smaller percentage of medulla volume in primates compared to insectivores ($F_{1,75} = 342.53$, $p < 0.001$). Total orofacial motor nucleus volume occupies 1.03% of medulla volume in insectivores and 0.44% of medulla volume in primates on average. This resembles the sensory trigeminal complex, which also forms a larger percentage of medulla volume in insectivores compared to primates (Baron et al., 1990). The percentage of the

Table 2
Percentage of medulla volume comprised by orofacial motor nuclei

Taxon	N	Percentage of Medulla			
		Vmo	VII	XII	Total
INSECTIVORA	30	0.20	0.60	0.24	1.03
PRIMATES	47	0.13	0.17	0.14	0.44
Lemuroidea	11	0.14	0.19	0.19	0.52
Daubentoniidae	1	0.13	0.13	0.14	0.40
Indriidae	4	0.15	0.17	0.13	0.45
Lepilemuridae	1	0.15	0.20	0.26	0.61
Cheirogaleidae	3	0.14	0.25	0.26	0.65
Lemuridae	2	0.11	0.17	0.19	0.47
Lorisoidea	6	0.16	0.22	0.16	0.54
Galagonidae	3	0.14	0.26	0.15	0.55
Lorisidae	3	0.18	0.19	0.17	0.54
Tarsioidea	1	0.18	0.36	0.13	0.67
Ceboidea	13	0.13	0.13	0.12	0.38
Cebidae	8	0.13	0.14	0.13	0.40
Atelidae	5	0.12	0.12	0.11	0.36
Cercopithecoidea	10	0.12	0.16	0.10	0.37
Hominoidea	6	0.09	0.17	0.14	0.40

Primate nucleus volumes are from only the left side. Insectivore data are taken from Stephan et al. (1991) and divided by two to arrive at the volume of single nuclei. N = number of species.

medulla occupied by the orofacial motor nuclei is smaller in haplorhines (0.39%) compared to strepsirrhines (0.53%) ($F_{1,45} = 26.12$, $p < 0.001$), though there is considerable variation within each taxon. It should be noted, however, that although such percentages may suggest certain trends, they are strongly affected by the reference volume. Thus, the relatively smaller size of the orofacial motor nuclei in primates compared to insectivores may be due to enlargement of other structures of the medulla such as the pyramidal tract (Verhaart, 1970) and the inferior olivary nucleus (Stephan et al., 1991).

Volumetric data—scaling relationships

To evaluate relative rates of volumetric change among the orofacial motor nuclei, the volume of each nucleus was regressed against the volume of the other two (Table 3). For example, the volume of Vmo was regressed on the combined volume of VII and XII. For all nuclei, both LS and RMA slopes for nonphylogenetic regressions contain 1 within their 95% confidence intervals, indicating scaling isometry. When these scaling relationships were reanalyzed with ICs to control for phylogenetic bias in the data, LS and RMA slopes remain very close to 1.

Table 4 presents the results of the analysis of phylogenetic signal. The *K*-value for medulla volume is larger than 1, indicating that close relatives are more similar in medulla volume than expected by Brownian motion evolution. In contrast, the *K*-values for Vmo, VII, and XII are less than 1. Blomberg et al. (2003) found that, besides body size, most traits have *K*-values of less than 1. Such *K*-values may be caused by deviations from expected Brownian motion character evolution, such as adaptation within a subset of species, and/or measurement error of the tip data, branch lengths, or tree topology. Overall, in comparison to other traits examined by Blomberg et al. (2003), the orofacial motor nucleus volumetric data do not deviate to a great extent from expected levels of phylogenetic signal.

The influence of phylogenetic bias on the scaling relationship between the volume of orofacial motor nuclei against the medulla was determined by examining nonphylogenetic LS

Table 3
Coefficients for the log-log regression of the volume of each orofacial motor nucleus versus the others (N = 47)

Nucleus	Nonphylogenetic (species values)								Phylogenetic (independent contrasts)			
	r	p	LS			RMA			r	p	LS slope	RMA slope
			slope	95% CI		slope	95% CI					
Vmo	0.965	0.000	0.948	0.871	1.026	0.994	0.937	1.051	0.953	0.000	1.021	1.071
VII	0.971	0.000	1.014	0.938	1.089	1.044	0.969	1.120	0.946	0.000	0.919	0.971
XII	0.968	0.000	0.969	0.894	1.044	1.001	0.925	1.076	0.956	0.000	0.979	1.024

Table 4
Quantification of the strength of phylogenetic signal (K)

Trait	Observed MSE_0/MSE	K
Medulla volume	3.004	1.139
Vmo volume	2.122	0.805
VII volume	2.476	0.939
XII volume	2.335	0.886
Vmo GLI	1.240	0.470
VII GLI	1.092	0.414
XII GLI	1.563	0.593

For a detailed explanation of this method, see Blomberg et al. (2003). In brief, the observed MSE_0/MSE is the ratio of the mean squared error of the tip data, measured from the phylogenetically corrected mean (MSE_0), divided by the mean squared error of the data calculated using the variance–covariance matrix derived from the specified tree (MSE). This value is then scaled by dividing it by the expected MSE_0/MSE under Brownian motion evolution along the specified tree topology. The expected MSE_0/MSE for the tree used in our analyses is 2.637. The amount of phylogenetic signal is measured as:

$$K = \frac{\text{observed } MSE_0/MSE}{\text{expected } MSE_0/MSE}$$

regression slopes in comparison to slopes calculated with ICs. The significance of the phylogenetic effect was assessed by determining whether the slope of IC lines fall within the 95% confidence limits of the slope of the nonphylogenetic regression. Several regressions were calculated based on different sets of ICs. It has been recognized that ICs between lower taxonomic levels may contain "noise" due to measurement or sampling error and hence might have undue influence on the estimation of scaling exponents (Purvis and Rambaut, 1995). This can be particularly problematic when two taxa that have diverged relatively recently differ markedly. In this situation, ICs are exaggerated by their shorter branch lengths. In our dataset, this type of sampling error was particularly evident for the IC at the stem galagid node. Due to the large brain and body size of *Otolemur crassicaudatus* compared to *Galago senegalensis* and *Galagoides demidoff*, the IC at the stem galagid node was an outlier in all scatterplots. Due to the leverage of this contrast on scaling coefficients, regressions were recalculated after removing the stem galagid IC. Another way to correct for the error in contrasts along more recent branches is to divide ICs into separate subgroups according to the depth or age of nodes in the tree and to analyze only contrasts that represent the nodes between higher-order taxa (Purvis and Rambaut, 1995; Deaner et al., 2002). These higher-order ICs include data from several species, so noise at the tips of the tree will tend to be averaged out. Therefore, we also calculated regressions from only nodes corresponding to contrasts between taxonomic ranks including subfamilies and higher.

Table 5 shows statistics for the LS regression of orofacial motor nucleus volumes versus medulla volume using species values, all ICs, ICs excluding the stem galagid contrast, and only higher-order ICs. The volume of each nucleus is strongly positively correlated with medulla volume for all analyses. For Vmo, two out of three IC slopes exceed the confidence limits of the nonphylogenetic line. However, the greatest deviation from the nonphylogenetic slope is the regression of all ICs, where the stem galagid contrast exerts greater leverage than any other point. With this point removed, the Vmo regression slope is similar to the nonphylogenetic line. In addition, the higher-order ICs slope is very close to the upper limit of the nonphylogenetic LS confidence interval, suggesting that phylogenetic effects are small. For both VII and XII, one out of three IC slopes is significantly different from the nonphylogenetic LS regression line. These results underscore the sensitivity of IC-based regressions to the composition of the comparative sample. Taken together, these results suggest that phylogenetic relatedness does not exert consistent disproportionate leverage on the scaling of orofacial motor nuclei against medulla.

Both nonphylogenetic and phylogenetic slopes indicate that volumes of orofacial motor nuclei hyposcale with respect to medulla volume across primates. Slopes of nonphylogenetic LS regressions range from 0.861 to 0.888 and do not include 1 in their confidence limits. Phylogenetic slopes, except for the regression of Vmo for all ICs, are also lower than 1. In sum, the volume of orofacial motor nuclei does not keep pace with increases in total medulla volume.

Table 5
Comparison of correlation coefficients and slopes for different scaling analyses of orofacial motor nucleus volumes against medulla volume

Nucleus	Method	N	r	p	slope	95% CI	
Vmo	Nonphylogenetic LS	47	0.984	0.000	0.872	0.825	0.919
	Nonphylogenetic RMA	47	0.984	0.000	0.886		
	Phylogenetic LS (all ICs)	46	0.902	0.000	**1.100**		
	Phylogenetic LS (excluding stem galagid IC)	45	0.822	0.000	0.846		
	Phylogenetic LS (higher-order ICs only)	16	0.895	0.000	**0.922**		
VII	Nonphylogenetic LS	47	0.963	0.000	0.888	0.813	0.963
	Nonphylogenetic RMA	47	0.963	0.000	0.923		
	Phylogenetic LS (all ICs)	46	0.845	0.000	0.875		
	Phylogenetic LS (excluding stem galagid IC)	45	0.722	0.000	**0.733**		
	Phylogenetic LS (higher-order ICs only)	16	0.714	0.002	0.907		
XII	Nonphylogenetic LS	47	0.959	0.000	0.861	0.784	0.937
	Nonphylogenetic RMA	47	0.959	0.000	0.898		
	Phylogenetic LS (all ICs)	46	0.855	0.000	**0.940**		
	Phylogenetic LS (excluding stem galagid IC)	45	0.758	0.000	0.869		
	Phylogenetic LS (higher-order ICs only)	16	0.667	0.005	0.797		

Boldface type indicates slopes that exceed the 95% confidence intervals (CI) of the nonphylogenetic LS slope.

Volumetric data—grade shifts and allometric departures

Vmo volume

The double logarithmic scatterplot of Vmo volume versus medulla volume is shown in Fig. 5a. In many allometric relationships, a "grade shift" exists wherein the scaling exponent is the same across different higher-order taxa but the intercept is displaced in elevation. Grade shifts correspond to evolutionary events where a significant change in the relative size of structures has occurred at the base of a lineage and this reorganized relationship between structures is found in all descendents across variation in size. As a first approach in analyzing phylogenetic specializations, species values were analyzed using standard methods for detecting grade shifts by analysis of covariance (ANCOVA). If regression slopes were not found to differ, then parallel LS regression lines were fit to each clade and tested for differences in y-intercept.

Separate regression lines fit through strepsirrhines and haplorhines (Fig. 5b) do not differ significantly in slope ($t = 2.10$, $p = 0.156$) and after fitting parallel lines through each clade, intercepts also do not differ ($t = 2.00$, $p = 0.129$), indicating that a grade shift does not exist. Grade shifts can also be tested directly from ICs by demonstrating that the contrast between two taxa is a significant outlier and the slopes of the two grades are parallel by ANCOVA through the origin (Purvis and Rambaut, 1995). The scatterplot of ICs shows that the strepsirrhine-haplorhine contrast is not an outlier (Fig. 5c). Several contrasts at internal nodes of the tree, however, deviate significantly from allometric expectations as indicated in Fig. 5c. We did not evaluate grade shifts at internal nodes by fitting parallel slopes because of the small number of contrasts in each clade.

Because there was a relatively minimal phylogenetic effect on the scaling of Vmo against medulla, the nonphylogenetic regression line can be taken as a reasonable estimate of the changes in Vmo volume required to maintain functional equivalence with changes in medulla volume. Therefore, species-specific deviations from allometric expectations were evaluated based on the nonphylogenetic LS regression. Based on this reference line, *Nycticebus coucang*, *Macaca mulatta*, and *Pan paniscus* are significant outliers, i.e., with studentized deleted residuals (SDR) greater than 2 or less than −2. To represent volumetric changes in these species in more intuitive terms, we calculated a prediction difference (PD) between

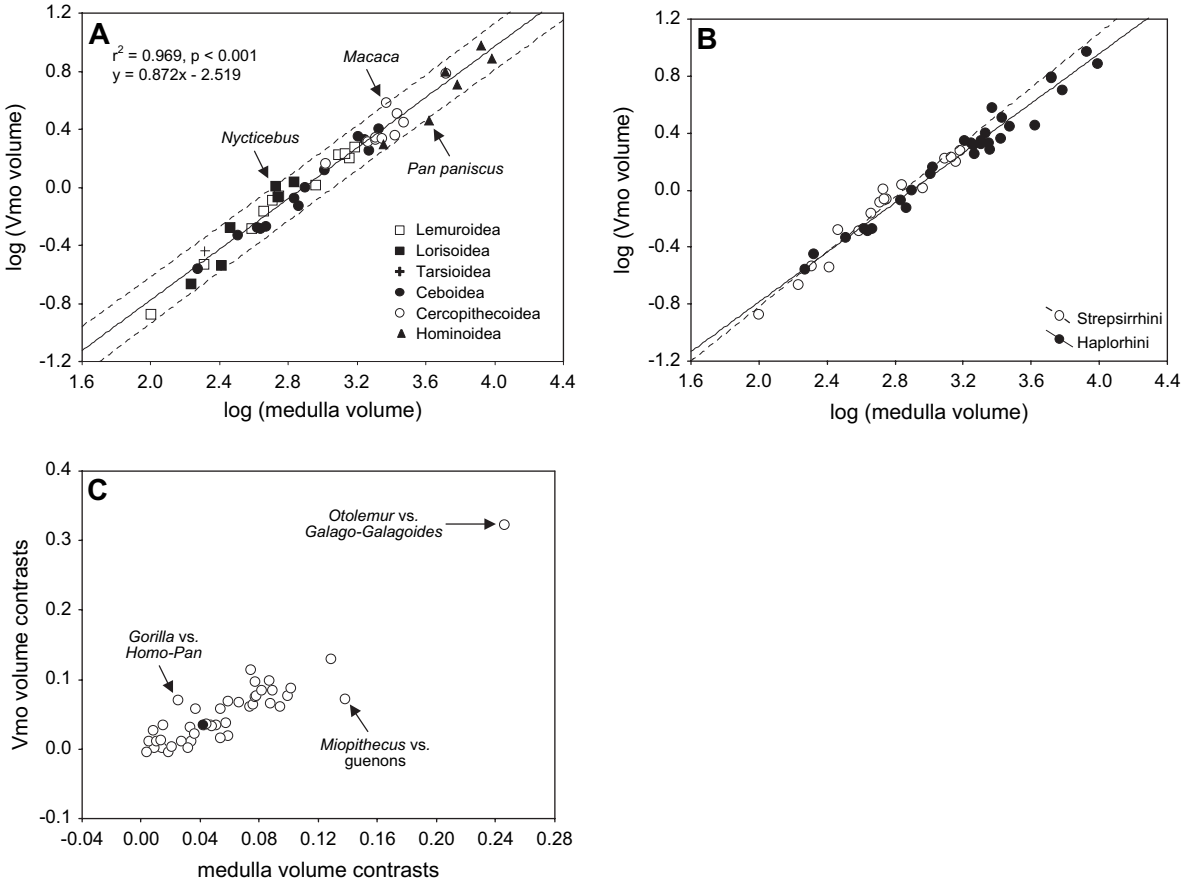

Fig. 5. Scaling analysis of Vmo volume versus medulla volume in primates. (a) A least-squares regression line is fit to the entire primate sample with 95% prediction intervals shown. (b) Separate least-squares regression lines are fit through strepsirrhines and haplorhines. (c) Independent contrasts showing the strepsirrhine-haplorhine contrast (black dot) and indicating the other contrasts that were significant outliers from the least-squares regression of all ICs.

observed and predicted nucleus volume in these taxa from the nonphylogenetic regression. To calculate the PD, a prediction was obtained based on the log-log LS regression. This predicted value was then detransformed from logarithmic units back to the arithmetic scale and the quasi-maximum likelihood estimator (e.g., Smith, 1993) was applied as a correction factor for detransformation bias. Finally, the ratio of (observed − predicted)/observed was calculated. Table 6 shows PDs and SDRs for Vmo volume in each species based on the nonphylogenetic common primate regression line. The volume of Vmo in *Nycticebus coucang* is 31% greater than predicted (SDR = 2.25) for a primate of the same medulla volume, *Macaca mulatta* is 32% greater than predicted (SDR = 2.37), and *Pan paniscus* is 50% less than predicted (SDR = −2.55).

VII volume

The double logarithmic scatterplot of VII volume versus medulla volume is shown in Fig. 6a. Separate regression lines fit through strepsirrhine and haplorhine species values (Fig. 6b) have significantly different slopes ($t = 6.00$, $p = 0.018$), with a steeper slope for haplorhines (slope = 0.990, SE = 0.052, 95% CI = 0.883, 1.097) compared to strepsirrhines (slope = 0.767, SE = 0.042, 95% CI = 0.678, 0.857). Since these LS lines are not parallel, they

Table 6
Prediction difference (PD) and standardized deleted residuals (SDR) for each species from nonphylogenetic least-squares regressions of orofacial motor nucleus volumes against medulla volumes based on the common primate line

Species	Vmo volume		VII volume		XII volume	
	PD	SDR	PD	SDR	PD	SDR
Microcebus murinus	−0.24	−1.32	0.27	1.24	0.25	1.10
Cheirogaleus major	−0.04	−0.21	0.10	0.36	0.36	1.66
Cheirogaleus medius	−0.05	−0.28	0.23	0.96	0.41	1.98
Eulemur fulvus	−0.10	−0.57	−0.10	−0.34	0.18	0.72
Varecia variegata	−0.06	−0.32	0.14	0.56	0.42	2.00
Lepilemur ruficaudatus	0.10	0.59	0.10	0.39	0.41	1.99
Avahi laniger laniger	0.15	0.94	0.08	0.32	−0.10	−0.32
Avahi laniger occidentalis	0.16	1.01	−0.12	−0.41	−0.21	−0.67
Propithecus verreauxi	0.11	0.69	−0.01	−0.04	0.01	0.05
Indri indri	0.06	0.34	0.12	0.46	0.06	0.22
Daubentonia madagascariensis	0.06	0.34	−0.20	−0.67	0.12	0.46
Loris tardigradus	0.21	1.41	0.02	0.09	0.03	0.10
Nycticebus coucang	0.31	2.25	0.01	0.04	−0.02	−0.05
Perodicticus potto	0.19	1.25	0.08	0.32	0.25	1.02
Galago senegalensis	−0.31	−1.62	0.17	0.68	−0.18	−0.60
Otolemur crassicaudatus	0.16	1.03	0.32	1.43	0.02	0.09
Galagoides demidoff	−0.21	−1.14	0.29	1.28	−0.04	−0.14
Tarsius syrichta	0.13	0.82	0.45	2.38	−0.25	−0.81
Callithrix jacchus	0.02	0.14	−0.11	−0.38	−0.13	−0.44
Cebuella pygmaea	−0.03	−0.18	−0.40	−1.27	−0.13	−0.46
Saguinus midas	−0.15	−0.81	−0.23	−0.77	−0.15	−0.50
Saguinus oedipus	−0.08	−0.43	−0.53	−1.58	−0.01	−0.04
Callimico goeldii	−0.16	−0.89	−0.72	−2.06	−0.27	−0.85
Cebus albifrons	0.06	0.36	−0.10	−0.34	−0.09	−0.31
Aotus trivirgatus	−0.04	−0.21	0.06	0.21	−0.10	−0.33
Callicebus moloch	−0.01	−0.07	−0.14	−0.46	−0.11	−0.38
Saimiri sciureus	−0.25	−1.29	−0.48	−1.45	−0.24	−0.77
Pithecia monachus	0.05	0.27	−0.25	−0.81	0.00	0.01
Alouatta seniculus	0.17	1.09	−0.46	−1.38	−0.24	−0.77
Ateles geoffroyi	−0.18	−0.96	−0.73	−2.07	−0.27	−0.86
Lagothrix lagothricha	0.06	0.37	−0.20	−0.67	−0.20	−0.65
Macaca mulatta	0.32	2.37	0.28	1.23	0.28	1.18
Lophocebus albigena	0.10	0.60	0.08	0.29	−0.02	−0.08
Papio anubis	0.15	0.96	0.04	0.15	−0.20	−0.66
Cercopithecus ascanius	−0.01	−0.05	−0.06	−0.21	−0.12	−0.40
Cercopithecus mitis	−0.07	−0.38	0.00	0.00	−0.18	−0.59
Miopithecus talapoin	0.12	0.75	0.08	0.29	−0.13	−0.44
Erythrocebus patas	−0.24	−1.30	0.15	0.59	−0.28	−0.89
Procolobus badius	−0.03	−0.16	−0.36	−1.14	−0.63	−1.79
Pygathrix nemaeus	−0.15	−0.80	−0.20	−0.68	−0.70	−1.96
Nasalis larvatus	−0.14	−0.77	0.02	0.06	−0.57	−1.65
Hylobates lar	−0.30	−1.55	−0.66	−1.90	−0.11	−0.37
Pongo pygmaeus	0.17	1.11	0.44	2.28	0.54	3.15
Gorilla gorilla	0.16	1.04	0.17	0.71	0.18	0.72
Pan troglodytes	−0.18	−0.99	0.33	1.56	0.20	0.80
Pan paniscus	−0.50	−2.55	0.21	0.90	−0.12	−0.41
Homo sapiens	−0.17	−0.98	0.03	0.13	0.34	1.58

PD = (observed − predicted)/observed.

were not tested further for differences in intercept. Furthermore, the scatterplot of ICs shows that the strepsirrhine-haplorhine contrast is not a significant outlier (Fig. 6c). Examination of the location of internal nodes on the scatterplot of ICs reveals that the contrast between *Hylobates lar* and hominids (i.e., great apes and humans) is a significant outlier from the LS regression (SDR = 3.05), suggesting that a significant change in VII volume occurred at this node.

To investigate the nature of VII volume change at the node between hylobatids and hominids, a LS prediction equation was calculated based on data from all haplorhine individuals excluding hominids (Fig. 6d). Compared to this regression function, 14 out of 15 observed values for hominid individuals are greater than predicted, however only two individuals have VII volumes that exceed the 95% prediction intervals. Another way to evaluate whether a group of points deviates from allometric predictions is to test if the average difference between observed and predicted values is significantly greater than zero by a paired samples *t*-test (Rilling and Seligman, 2002). Analyzed in this way, the observed VII volume of hominids is significantly larger than predicted for nonhominid haplorhines of their medulla volume (paired *t*-test: $t = 5.27$, $p < 0.001$, d.f. = 14).

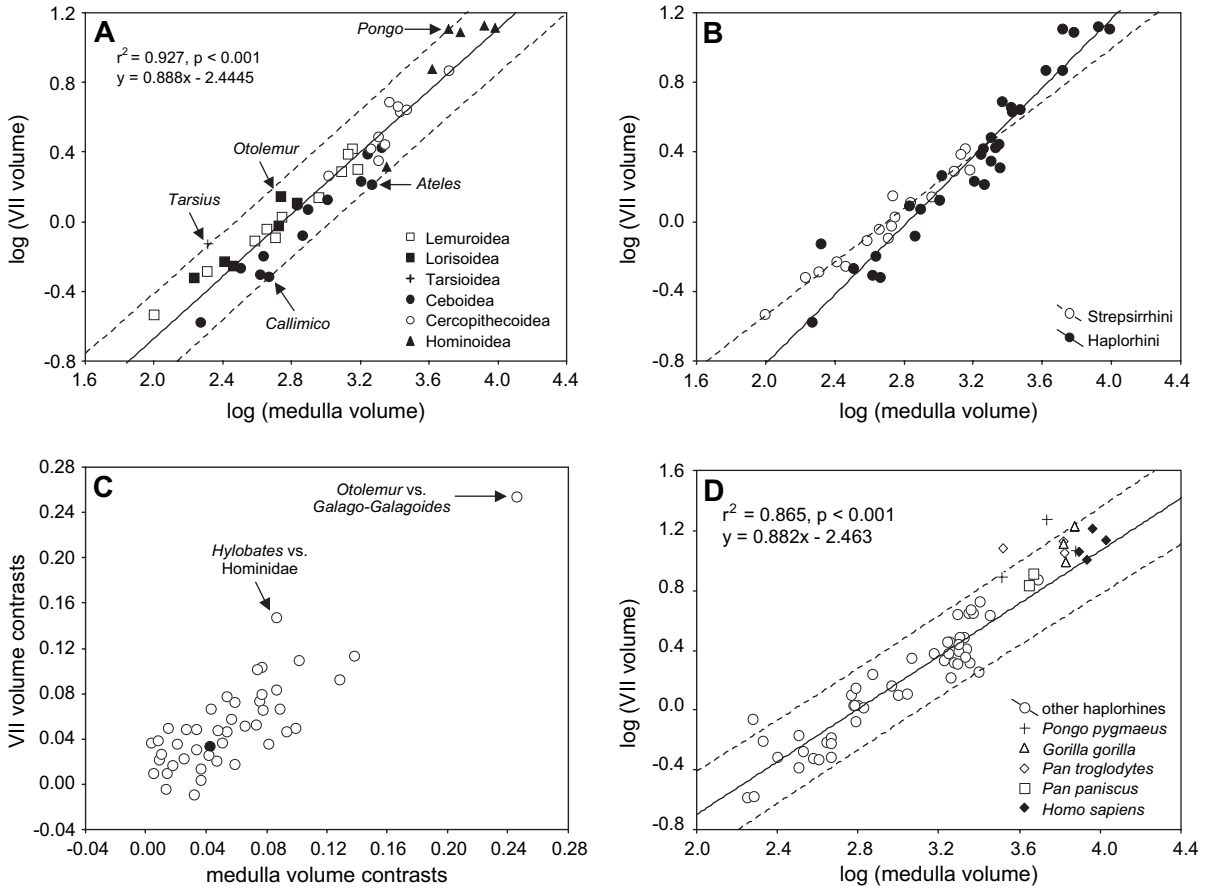

Fig. 6. Scaling analysis of VII volume versus medulla volume in primates. (a) A least-squares regression line is fit to the entire primate sample with 95% prediction intervals shown. (b) Separate least-squares regression lines are fit through strepsirrhines and haplorhines. (c) Independent contrasts showing the strepsirrhine-haplorhine contrast (black dot) and indicating the other contrasts that were significant outliers from the least-squares regression of all ICs. (d) The least-squares regression line and associated 95% prediction intervals were calculated from non-hominid haplorhine individuals. Hominid data points are plotted with respect to the prediction line.

Table 6 shows PDs and SDRs for VII volume in each species based on the nonphylogenetic common primate regression line. Based on this function, VII volume of *Tarsius syrichta* is 45% greater than predicted (SDR = 2.38), *Callimico goeldii* is 72% less than predicted (SDR = −2.06), *Ateles geoffroyi* is 73% less than predicted (SDR = −2.07), and *Pongo pygmaeus* is 44% greater than predicted (SDR = 2.28). Because strepsirrhine and haplorhine lines have significantly different slopes, species-specific departures from allometry were also tested based on the appropriate suborder regression. This is important since prediction equations can be sensitive to the taxonomic composition of the reference group (Holloway and Post, 1982; Harvey and Krebs, 1990). Based on the separate suborder prediction equations, VII volume of *Otolemur crassicaudatus* is 25% greater than predicted (SDR = 2.66) for a strepsirrhine of its medulla volume and *Tarsius syrichta* is 58% greater than predicted (SDR = 3.99) for a haplorhine of its medulla volume. Due to the controversial phylogenetic position of tarsiers, the *Tarsius* datapoint was retested to determine whether it departs significantly from allometric expectations when prosimians are used as the reference group. *Tarsius* had a 29% larger VII than predicted for its medulla volume (SDR = 2.77) on the basis of the prosimian regression line. It is worth noting that the tarsier point falls closer to the prosimian regression than the haplorhine regression, suggesting that *Tarsius* is more prosimian-like in this trait.

XII volume

The double logarithmic scatterplot of XII volume versus medulla volume is shown in Fig. 7a. Separate regression lines fit through the species values for the two primate suborders (Fig. 7b) do not differ in slope ($t = 1.00$, $p = 0.317$). However, after fitting parallel lines through each group, the strepsirrhine regression has a significantly higher elevation ($t = 13.10$, $p = 0.001$). This finding indicates that either XII is relatively reduced in haplorhines or other components of the medulla are larger in haplorhines as compared to strepsirrhines. These possibilities merit further investigation in future studies. The scatterplot of ICs, however, suggests that the strepsirrhine-haplorhine contrast is not a significant outlier (Fig. 7c).

Table 6 shows PDs and SDRs for XII volume in each species based on the nonphylogenetic common primate regression line. Based on this regression, XII volume of *Varecia variegata* is 42% greater (SDR = 2.00) and *Pongo pygmaeus* is 54% greater than predicted (SDR = 3.15). Because strepsirrhine and haplorhine regression lines have significantly different elevations, species-specific departures from allometry were also tested based on the appropriate suborder regression line. Based on these prediction equations, XII volume of *Pygathrix nemaeus* is 61% smaller (SDR = −2.01) and *Pongo pygmaeus* is 53% greater than predicted (SDR = 3.81) for haplorhines of their medulla volume.

There has been recent interest concerning the role of tongue innervation in the evolution of human speech abilities (Kay et al., 1998; DeGusta et al., 1999; Jungers et al., 2003). Therefore, we tested the hypothesis that XII volume may be enlarged in humans by analyzing the size and scaling of this nucleus among the individual specimens in our sample. Fig. 8 shows the distribution of XII volumes across primates. In absolute size, humans have the largest XII among primates (mean = 14.39 mm^3, n = 4), significantly larger than XII volume in the pooled great ape sample ($t = -2.66$, $p = 0.020$, d.f. = 13). Several human values, however, overlap with the range of XII volumes in both orang-utans and gorillas.

Next, we examined whether human XII volumes are predicted by allometric scaling based on medulla volume in nonhuman primates. Because we found a grade effect for XII volume scaling between primate suborders, we used only nonhuman haplorhine data in our prediction model. When plotted on this line (Fig. 7d), the human data points are observed above the regression function but within its prediction intervals. Although the volume of the human XII is 24% ± 9% (n = 4) larger than expected for a nonhuman haplorhine of the same medulla volume, the observed human values do not differ significantly from their predicted values (paired *t*-test: $t = 2.87$, $p = 0.064$, d.f. = 3). Of significance, the

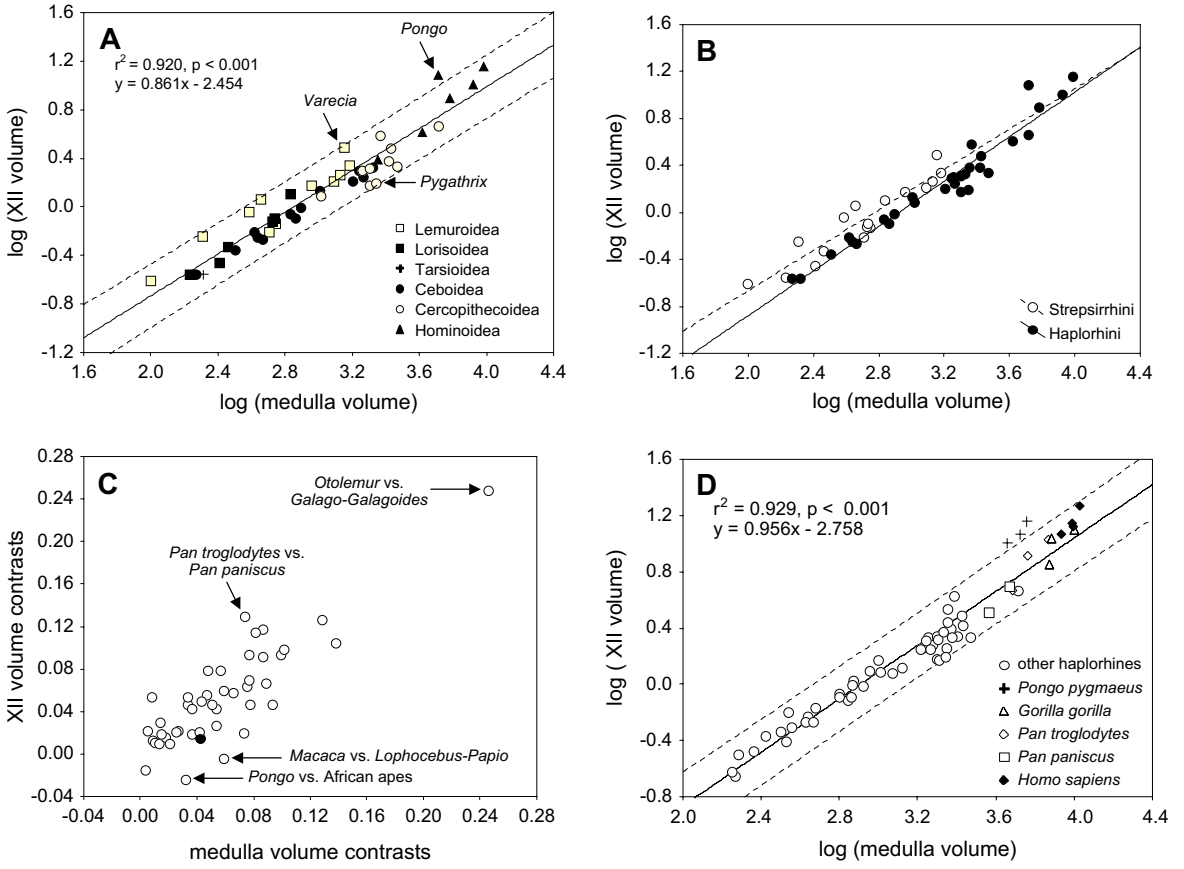

Fig. 7. Scaling analysis of XII volume versus medulla volume in primates. (a) A least-squares regression line is fit to the entire primate sample with 95% prediction intervals shown. (b) Separate least-squares regression lines are fit through strepsirrhines and haplorhines. (c) Independent contrasts showing the strepsirrhine-haplorhine contrast (black dot) and indicating the other contrasts that were significant outliers from the least-squares regression of all ICs. (d) The least-squares regression line and associated 95% prediction intervals were calculated from non-human haplorhine individuals. Human data points are plotted with respect to the prediction line.

volume of XII in *Pongo pygmaeus* is 51% ± 4% ($n = 3$) larger than predicted by the nonhuman haplorhine regression line and all data points from this species fall above the 95% prediction intervals. No other species data points exceed the prediction intervals of the LS regression line.

Grey Level Index—absolute values

Species mean GLI values are shown in Table 7. Fig. 9 displays the mean GLI for each nucleus by superfamily. One-way ANOVA was performed on GLIs with superfamily as a factor (excluding tarsioids because of small sample size). For each nucleus, there is a significant effect of superfamily in the ANOVA model (Fig. 9). Post hoc Bonferroni contrasts revealed a consistent trend for lorisoids to have significantly higher GLI values than other taxa across all nuclei. This is especially striking considering that the overall size of orofacial motor nuclei in lorisoids is very similar to that of lemuroids (Fig. 4).

Grey Level Index—scaling relationships

The *K* statistics for GLI data are presented in Table 4. *K*-values for GLIs are all less than 1 and are substantially lower than *K*-values for volumetric

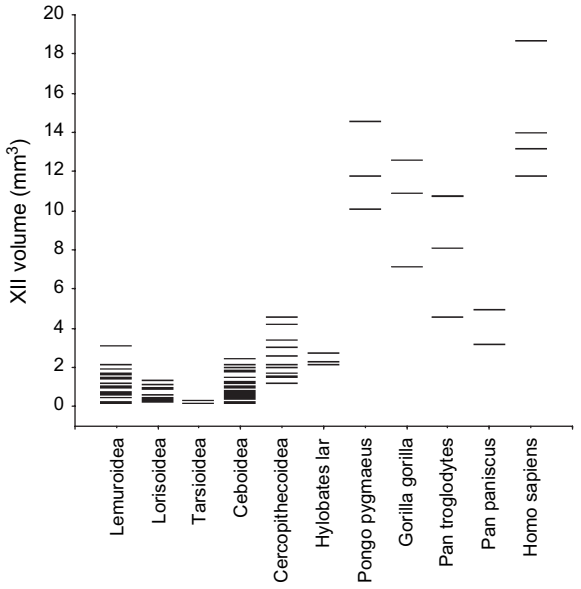

Fig. 8. XII volumes from each individual included in this study.

data, indicating that GLIs have less phylogenetic signal than nucleus volumes. In other words, GLIs tend be less similar among closely related species than expected under Brownian motion evolution, whereas motor nucleus volumes fall closer to their expected values based on phylogenetic signal. Next, the influence of phylogenetic bias on the scaling of GLI versus nucleus volume (cube root) was determined by examining nonphylogenetic LS regression slopes in comparison to IC slopes. Table 8 shows statistics for the LS regression of GLIs versus nucleus volumes using species values, all ICs, ICs excluding the galagid contrast, and only higher-order ICs. The GLI of each nucleus is significantly negatively correlated with nucleus volume in all analyses except those using higher-order ICs and ICs excluding the stem galagid contrast for VII. The effect of phylogenetic bias on scaling was examined for those regressions that were statistically significant. In several cases, phylogenetic slopes are significantly more negative than slopes based on species values. However, all IC slopes are not consistently different from nonphylogenetic slopes for any nucleus. Thus, similar to our volumetric results, these findings point to the sensitivity of phylogenetic regression methods to the composition of the sample. Furthermore, the incongruity of nonphylogenetic and phylogenetic slopes for GLIs accords with the consistently lower K statistics for GLI data compared to volumetric data.

Grey Level Index—grade shifts and allometric departures

Vmo GLI

The double logarithmic scatterplot of Vmo GLI scaling against Vmo volume (cube root) is shown in Fig. 10a. Separate regression lines fit through strepsirrhine and haplorhine species values (Fig. 10b) do not have significantly different slopes ($t = 0.23$, $p = 0.632$) or intercepts ($t = 0.17$, $p = 0.686$). In addition, the strepsirrhine-haplorhine contrast is not an outlier in the scatterplot of ICs (Fig. 10c).

Table 9 shows PDs and SDRs for Vmo GLI in each species based on the nonphylogenetic common primate regression line. According to this function, Vmo GLI in *Papio anubis* is 147% less than predicted for its Vmo volume (SDR = −3.70) and Vmo GLI in *Pongo pygmaeus* is 49% higher than predicted (SDR = 2.61).

VII GLI

The double logarithmic scatterplot of VII GLI scaling on VII volume (cube root) is shown in Fig. 11a. Separate regression lines fit through strepsirrhine and haplorhine species values (Fig. 11b) do not have significantly different slopes ($t = 2.44$, $p = 0.126$) or intercepts ($t = 0.19$, $p = 0.666$). The scatterplot of ICs supports this result, with the strepsirrhine-haplorhine not being an outlier (Fig. 11c).

Table 9 shows PDs and SDRs for VII GLI in each species based on the nonphylogenetic common primate regression line. According to the nonphylogenetic regression, VII GLI in *Nasalis larvatus* is 80% less than predicted for its VII volume (SDR = −2.00) and VII GLI in *Pongo pygmaeus* is 54% higher than predicted (SDR = 2.86).

To test the hypothesis that VII is reorganized in terms of GLI among hominids, a LS prediction equation was calculated based on data from all primate individuals excluding hominids (Fig. 11d). Both strepsirrhines and haplorhine data were used

Table 7
Species means and standard deviations for Grey Level Index (GLI) of orofacial motor nuclei

Species	N	Vmo GLI		VII GLI		XII GLI	
		Mean	SD	Mean	SD	Mean	SD
Microcebus murinus	5	21.82	5.09	16.33	3.80	17.18	2.87
Cheirogaleus major	2	12.85	1.63	10.61	1.30	11.68	1.60
Cheirogaleus medius	2	18.59	6.49	15.20	0.00	15.79	2.89
Eulemur fulvus	2	15.31	2.15	11.24	1.91	13.43	2.44
Varecia variegata	1	14.23	-	7.02	-	8.57	-
Lepilemur ruficaudatus	2	13.05	1.65	10.55	1.07	12.37	1.75
Avahi laniger laniger	2	21.50	1.56	15.65	2.10	19.67	3.72
Avahi laniger occidentalis	2	15.08	3.11	10.04	0.63	14.11	1.86
Propithecus verreauxi	2	11.10	1.35	9.10	0.93	13.76	1.44
Indri indri	2	12.26	0.37	9.20	0.86	12.18	0.15
Daubentonia madagascariensis	1	8.81	-	8.84	-	12.31	-
Loris tardigradus	2	24.42	4.73	18.89	1.87	29.35	3.43
Nycticebus coucang	2	22.63	3.71	22.31	-	25.10	0.90
Perodicticus potto	2	17.09	1.57	12.10	0.26	19.03	2.08
Galago senegalensis	1	21.65	-	23.56	-	29.41	-
Otolemur crassicaudatus	2	15.84	2.19	13.74	3.35	18.72	2.85
Galagoides demidoff	2	23.64	5.60	20.40	3.66	24.62	5.91
Tarsius syrichta	2	20.92	0.96	15.64	1.62	28.08	2.77
Callithrix jacchus	3	16.75	2.08	13.57	0.91	20.16	2.50
Cebuella pygmaea	2	17.93	3.18	15.82	3.09	18.33	1.35
Saguinus midas	2	21.88	2.31	18.53	0.84	21.92	0.75
Saguinus oedipus	3	17.35	3.69	15.19	3.04	16.56	1.50
Callimico goeldii	1	18.61	-	9.50	-	14.49	0.00
Cebus albifrons	2	7.77	0.77	7.77	0.74	13.29	0.96
Aotus trivirgatus	2	12.85	6.44	11.95	2.95	19.47	0.65
Callicebus moloch	2	21.57	2.11	19.46	0.16	23.40	1.36
Saimiri sciureus	1	10.95	-	7.38	-	11.56	-
Pithecia monachus	2	18.22	1.21	19.71	3.19	20.01	0.14
Alouatta seniculus	2	13.04	2.66	11.28	-	17.10	2.71
Ateles geoffroyi	1	13.09	-	9.69	-	12.56	-
Lagothrix lagothricha	3	11.95	0.91	9.57	2.30	11.65	2.90
Macaca mulatta	2	9.50	-	8.05	0.67	13.19	1.59
Lophocebus albigena	1	10.67	-	6.73	-	9.24	-
Papio anubis	1	3.37	-	4.64	-	8.73	-
Cercopithecus ascanius	2	12.84	3.13	11.99	2.31	15.32	1.12
Cercopithecus mitis	1	11.19	-	13.25	-	15.90	0.00
Miopithecus talapoin	2	9.39	5.10	9.95	1.75	14.10	2.25
Erythrocebus patas	2	11.77	-	11.03	0.84	14.34	1.83
Procolobus badius	2	7.69	3.48	7.33	2.97	9.16	3.01
Pygathrix nemaeus	1	9.66	-	8.34	-	12.97	-
Nasalis larvatus	1	6.44	-	4.85	-	7.65	-
Hylobates lar	2	19.71	6.45	10.34	0.60	13.33	3.78
Pongo pygmaeus	2	16.36	3.12	14.46	5.86	15.25	3.54
Gorilla gorilla	3	6.91	4.87	5.53	3.36	5.09	1.15
Pan troglodytes	3	11.10	6.06	7.25	5.47	9.22	3.45
Pan paniscus	2	13.99	2.74	12.20	0.65	11.27	0.85
Homo sapiens	4	7.37	1.96	6.47	1.46	7.78	3.81

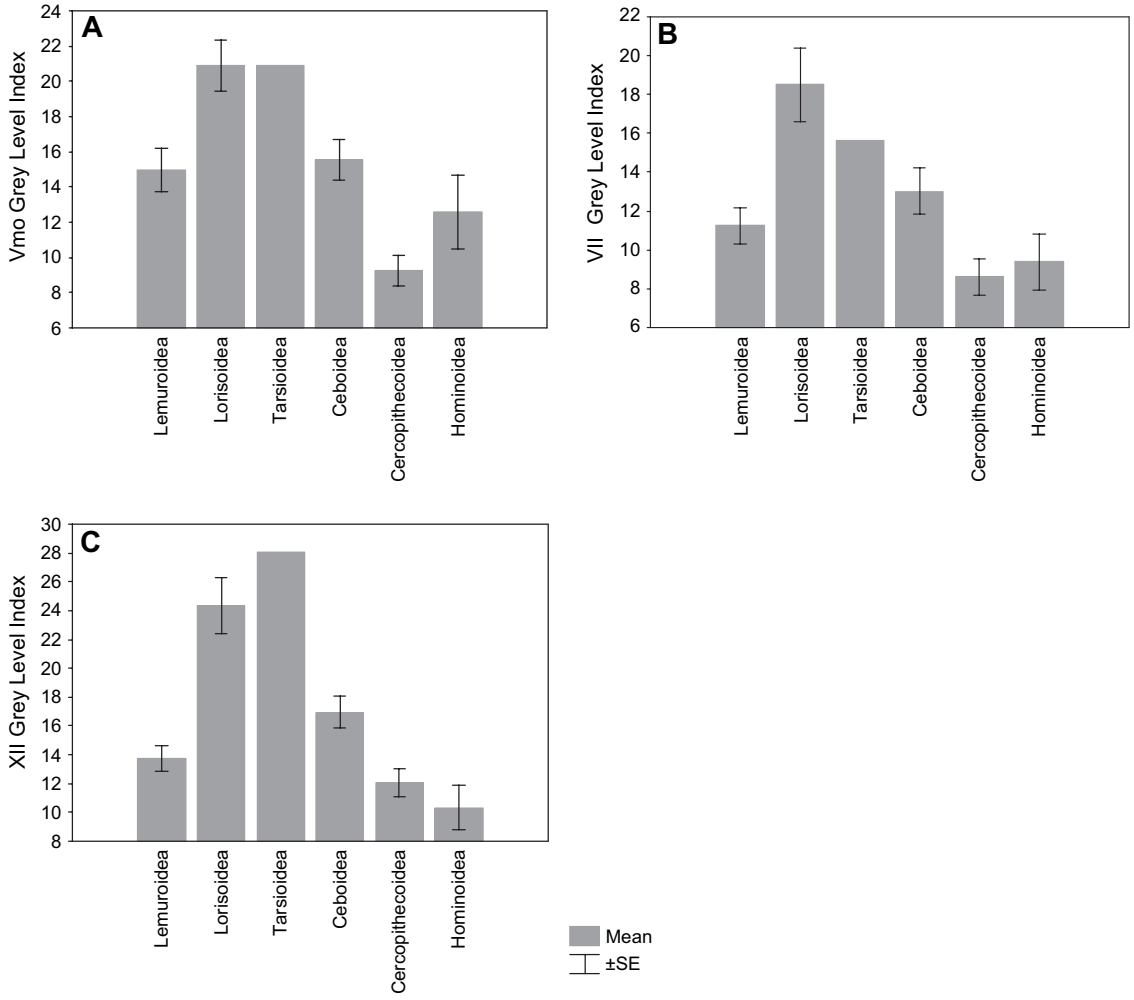

Fig. 9. Bar graphs of Grey Level Index of Vmo (a), VII (b), and XII (c) according to superfamily. One-way ANOVA of Vmo GLI with superfamily as a factor revealed a significant effect of phylogeny ($F_{5,41} = 7.55$, $p < 0.001$); Bonferroni post hoc analysis indicated that lorisoids have significantly higher GLIs than cercopithecoids ($p < 0.001$) and hominoids ($p = 0.012$). ANOVA of VII GLI also had a significant effect of superfamily ($F_{5,41} = 6.36$, $p < 0.001$); lorisoids had significantly higher GLIs than lemuroids ($p = 0.006$), cercopithecoids ($p < 0.001$), and hominoids ($p = 0.002$). ANOVA of XII GLI had a significant effect of superfamily ($F_{5,41} = 14.67$, $p < 0.001$); lorisoids had higher GLIs than all other superfamilies (Bonferroni post hoc, all comparisons $p < 0.01$), and ceboids had significantly higher GLIs than cercopithecoids ($p = 0.04$) and hominoids ($p = 0.01$).

to construct the prediction equation because there was no grade effect apparent on VII GLI scaling. Compared to this regression function, the observed VII GLI values for hominid individuals do not differ significantly from allometric predictions for primates of their VII volume (paired *t*-test: $t = 0.15$, $p = 0.886$, d.f. = 13).

XII GLI

The double logarithmic scatterplot of XII GLI scaling on XII volume (cube root) is shown in Fig. 12a. Separate regression lines fit through strepsirrhine and haplorhine species values (Fig. 12b) do not have significantly different slopes ($t = 0.93$, $p = 0.339$) or intercepts ($t = 0.00$,

Table 8
Comparison of correlation coefficients and slopes for different scaling analyses of orofacial motor nucleus GLI against nucleus volume (cube root)

Nucleus	Method	N	r	p	slope	95% CI	
Vmo	Nonphylogenetic LS	47	−0.719	0.000	−0.911	−1.175	−0.647
	Nonphylogenetic RMA	47	−0.719	0.000	**− 1.251**		
	Phylogenetic LS (all ICs)	46	−0.538	0.000	−1.093		
	Phylogenetic LS (excluding stem galagid IC)	45	−0.486	0.001	**− 1.459**		
	Phylogenetic LS (higher-order ICs only)	16	−0.225	0.402	**−0.529**		
VII	Nonphylogenetic LS	47	−0.642	0.000	−0.756	−1.027	−0.485
	Nonphylogenetic RMA	47	−0.642	0.000	**−1.178**		
	Phylogenetic LS (all ICs)	46	−0.429	0.003	**−1.041**		
	Phylogenetic LS (excluding stem galagid IC)	45	−0.206	0.180	−0.630		
	Phylogenetic LS (higher-order ICs only)	16	−0.133	0.624	**−0.281**		
XII	Nonphylogenetic LS	47	−0.737	0.000	−0.844	−1.076	−0.612
	Nonphylogenetic RMA	47	−0.737	0.000	**−1.144**		
	Phylogenetic LS (all ICs)	46	−0.491	0.001	−1.002		
	Phylogenetic LS (excluding stem galagid IC)	45	−0.332	0.028	−0.792		
	Phylogenetic LS (higher-order ICs only)	16	−0.464	0.070	**−1.143**		

Boldface type indicates slopes that exceed the 95% confidence intervals (CI) of the nonphylogenetic LS slope.

$p = 0.967$). Furthermore, the scatterplot of ICs shows that the strepsirrhine-haplorhine contrast is not a significant outlier (Fig. 12c).

Table 9 shows PDs and SDRs for XII GLI in each species based on the nonphylogenetic common primate regression line. According to this regression, XII GLI in *Nasalis larvatus* is 66% less than predicted for its XII volume (SDR = −2.08), *Gorilla gorilla* is 62% less than predicted (SDR = −2.06) and *Pongo pygmaeus* is 48% higher than predicted (SDR = 3.00).

To test whether the GLI of the human XII differs from allometric expectation, a LS prediction equation was calculated based on data from all primate individuals excluding humans (Fig. 12d). Compared to this regression function, the observed values for human individuals do not differ significantly from what is predicted for primates of their XII volume (paired *t*-test: $t = -0.09$, $p = 0.936$, d.f. = 3).

Socioecological correlations

Correlated evolution between orofacial motor nuclei and socioecological variables was tested using phylogenetic comparative methods. We hypothesized that a relationship might exist between (1) VII and sociality and (2) Vmo and diet. Independent contrasts were calculated for log-transformed nucleus volumes, GLIs, group size, and the percentage of leaves in the diet. Independent contrasts for nucleus volumes and GLIs were significantly correlated with ICs for medulla volume. Therefore, to adjust the data for overall size, residuals were calculated from LS regressions on medulla volume ICs. Group size ICs and percent folivory ICs were not correlated with medulla volume ICs, so they were not size-adjusted.

No correlation was found between size-adjusted VII volume ICs and group size ICs ($r = 0.046$, $p = 0.792$, $n = 38$) or size-adjusted VII GLI ICs and group size ICs ($r = -0.124$, $p = 0.471$, $n = 38$). In addition, there was no correlation between percent folivory in diet ICs and size-adjusted Vmo volume ICs ($r = -0.243$, $p = 0.213$, $n = 28$) or size-adjusted Vmo GLI ICs ($r = -0.045$, $p = 0.821$, $n = 28$).

Discussion

The volume and neuropil space (i.e., GLI) of orofacial cranial motor nuclei, Vmo, VII, and XII, were measured in a sample representing 47 primate species. The results of scaling analyses underscore

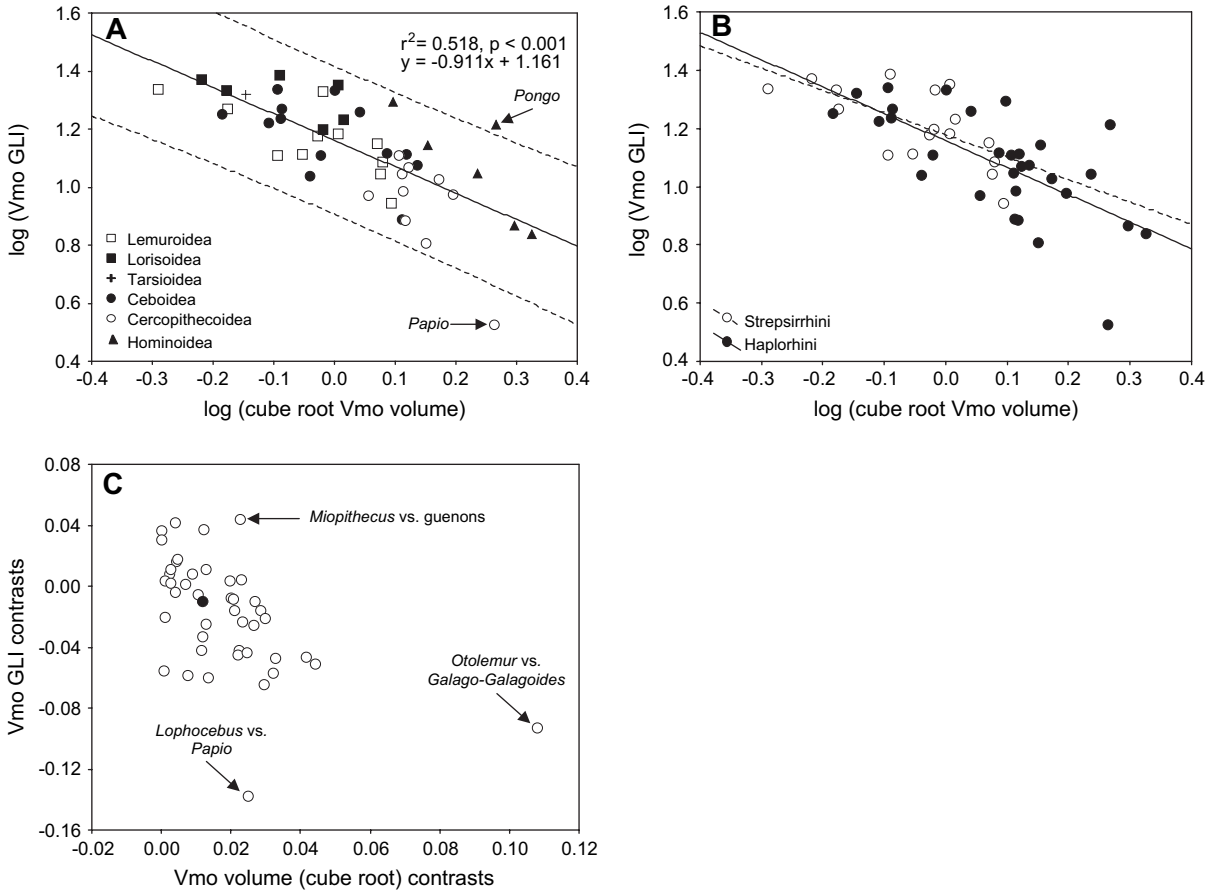

Fig. 10. Scaling analysis of Vmo GLI versus cube root Vmo volume in primates. (a) A least-squares regression line is fit to the entire primate sample with 95% prediction intervals shown. (b) Separate least-squares regression lines are fit through strepsirrhines and haplorhines. (c) Independent contrasts showing the strepsirrhine-haplorhine contrast (black dot) and indicating the other contrasts that were significant outliers from the least-squares regression of all ICs.

the tight interrelation among these nuclei with respect to one another and total medulla size. However, our analyses revealed several instances in which particular taxa depart from allometric predictions. As discussed below, these cases suggest that certain phylogenetic groups may have derived neural circuitry for orofacial motor adaptations in association with either elaboration of peripheral musculature and/or modifications of afferent connectivity.

Developmental considerations

Orofacial motor nucleus volumes were highly positively correlated with one another and with total medulla volume. Each nucleus scaled against the others with isometric slopes, indicating that changes in the size of orofacial motor nuclei are closely interlinked. In addition, orofacial motor nucleus volumes consistently hyposcaled with respect to total medulla volume due to a relatively greater rate of enlargement in other medullary components. Taken together, these findings show that developmental and allometric constraints are a significant determinant of the size of orofacial motor nuclei.

Although our data do not permit the direct examination of the proximate developmental mechanisms underlying these scaling patterns, it is informative to discuss our results in the context

Table 9
Prediction difference (PD) and standardized deleted residuals (SDR) for each species from nonphylogenetic least-squares regressions of orofacial motor nucleus GLI against nucleus volume (cube root) based on the common primate line

Species	Vmo GLI		VII GLI		XII GLI	
	PD	SDR	PD	SDR	PD	SDR
Microcebus murinus	−0.22	−0.74	−0.06	−0.19	−0.37	−1.29
Cheirogaleus major	−0.37	−1.13	−0.27	−0.79	−0.39	−1.30
Cheirogaleus medius	−0.13	−0.43	0.02	0.06	−0.17	−0.63
Eulemur fulvus	0.07	0.24	−0.04	−0.12	−0.05	−0.19
Varecia variegata	0.12	0.44	−0.41	−1.14	−0.34	−1.17
Lepilemur ruficaudatus	−0.24	−0.76	−0.23	−0.68	−0.23	−0.81
Avahi laniger laniger	0.30	1.25	0.20	0.75	0.12	0.51
Avahi laniger occidentalis	−0.02	−0.07	−0.33	−0.94	−0.28	−0.99
Propithecus verreauxi	−0.12	−0.38	−0.18	−0.52	−0.01	−0.02
Indri indri	0.00	−0.01	−0.10	−0.31	−0.10	−0.35
Daubentonia madagascariensis	−0.35	−1.06	−0.20	−0.61	−0.03	−0.12
Loris tardigradus	0.28	1.18	0.22	0.84	0.33	1.65
Nycticebus coucang	0.37	1.63	0.42	1.87	0.32	1.54
Perodicticus potto	0.18	0.68	0.02	0.06	0.22	1.00
Galago senegalensis	0.03	0.09	0.39	1.65	0.28	1.31
Otolemur crassicaudatus	0.05	0.17	0.15	0.55	0.10	0.42
Galagoides demidoff	0.03	0.11	0.25	0.97	0.08	0.34
Tarsius syrichta	0.06	0.21	0.13	0.45	0.19	0.86
Callithrix jacchus	−0.09	−0.29	−0.09	−0.28	0.01	0.05
Cebuella pygmaea	−0.19	−0.63	−0.12	−0.38	−0.24	−0.87
Saguinus midas	0.19	0.75	0.23	0.88	0.15	0.65
Saguinus oedipus	−0.01	−0.03	0.00	0.02	−0.09	−0.35
Callimico goeldii	0.06	0.23	−0.60	−1.60	−0.30	−1.03
Cebus albifrons	−0.48	−1.38	−0.30	−0.86	0.02	0.07
Aotus trivirgatus	−0.18	−0.58	0.00	−0.01	0.15	0.66
Callicebus moloch	0.33	1.41	0.38	1.57	0.32	1.54
Saimiri sciureus	−0.44	−1.29	−0.79	−1.99	−0.45	−1.49
Pithecia monachus	0.27	1.10	0.40	1.73	0.27	1.27
Alouatta seniculus	0.13	0.50	0.02	0.07	0.19	0.83
Ateles geoffroyi	0.07	0.27	−0.15	−0.46	−0.07	−0.27
Lagothrix lagothricha	0.09	0.32	−0.03	− 0.10	−0.10	−0.37
Macaca mulatta	−0.01	−0.05	−0.05	−0.17	0.18	0.78
Lophocebus albigena	0.05	0.19	−0.30	−0.88	−0.25	−0.89
Papio anubis	−1.47	−3.70	−0.65	−1.71	−0.18	−0.66
Cercopithecus ascanius	0.10	0.35	0.17	0.62	0.15	0.63
Cercopithecus mitis	−0.03	−0.09	0.28	1.08	0.19	0.82
Miopithecus talapoin	−0.37	−1.12	−0.09	−0.28	−0.06	−0.23
Erythrocebus patas	0.05	0.17	0.22	0.81	0.14	0.58
Procolobus badius	−0.48	−1.39	−0.41	−1.12	−0.54	−1.74
Pygathrix nemaeus	−0.18	−0.59	−0.17	−0.52	−0.08	−0.29
Nasalis larvatus	−0.64	−1.80	−0.80	−2.00	−0.66	−2.08
Hylobates lar	0.40	1.84	−0.02	−0.07	0.08	0.31
Pongo pygmaeus	0.49	2.61	0.54	2.86	0.48	3.00
Gorilla gorilla	−0.06	−0.21	−0.19	−0.61	−0.62	−2.06
Pan troglodytes	0.20	0.81	0.07	0.25	0.04	0.16
Pan paniscus	0.25	1.01	0.37	1.61	0.05	0.22
Homo sapiens	−0.06	−0.20	−0.03	−0.09	0.04	20.16

PD = (observed − predicted)/observed.

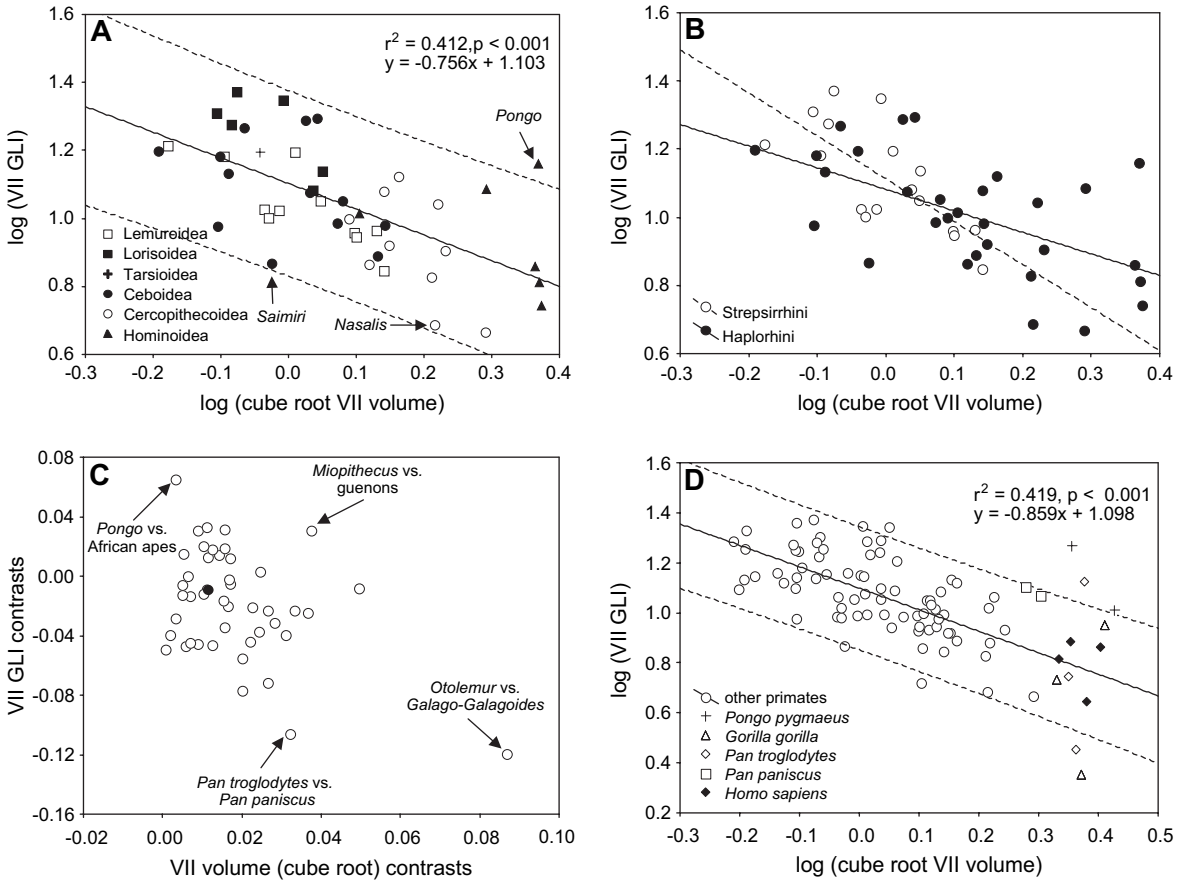

Fig. 11. Scaling analysis of VII GLI versus cube root VII volume in primates. (a) A least-squares regression line is fit to the entire primate sample with 95% prediction intervals shown. (b) Separate least-squares regression lines are fit through strepsirrhines and haplorhines. (c) Independent contrasts showing the strepsirrhine-haplorhine contrast (black dot) and indicating the other contrasts that were significant outliers from the least-squares regression of all ICs. (d) The least-squares regression line and associated 95% prediction intervals were calculated from non-hominid haplorhine individuals. Hominid data points are plotted with respect to the prediction line.

of processes that are known to control motoneuron survival and maturation. The number of motoneurons found in the adult motor nucleus is the result of initial proliferative events during neurogenesis and subsequent regressive events in the period of programmed cell death. In large part, extrinsic factors are involved in controlling the cell cycle dynamics of precursor populations. Molecules including basic fibroblast growth factor, transforming growth factor-α, insulin-like growth factor-I, and the monamine neurotransmitters stimulate proliferation, whereas glutamate, γ-aminobutyric acid, and opioid peptides down-regulate proliferation (Cameron et al., 1998). Approximately half of the motoneurons produced during neurogenesis undergo apoptosis. Motoneurons proceed through two distinct phases of programmed cell death during embryonic development. In the early phase, intrinsic cell-autonomous target-independent signals, such as $p75^{NTR}$ binding of nerve growth factor (NGF), are thought to regulate motoneuron survival (Sendtner et al., 2000). In the later phase, neurotrophic factors derived from skeletal muscles, Schwann cells, and afferent inputs have a significant effect on motoneuron survival (Sohal et al.,

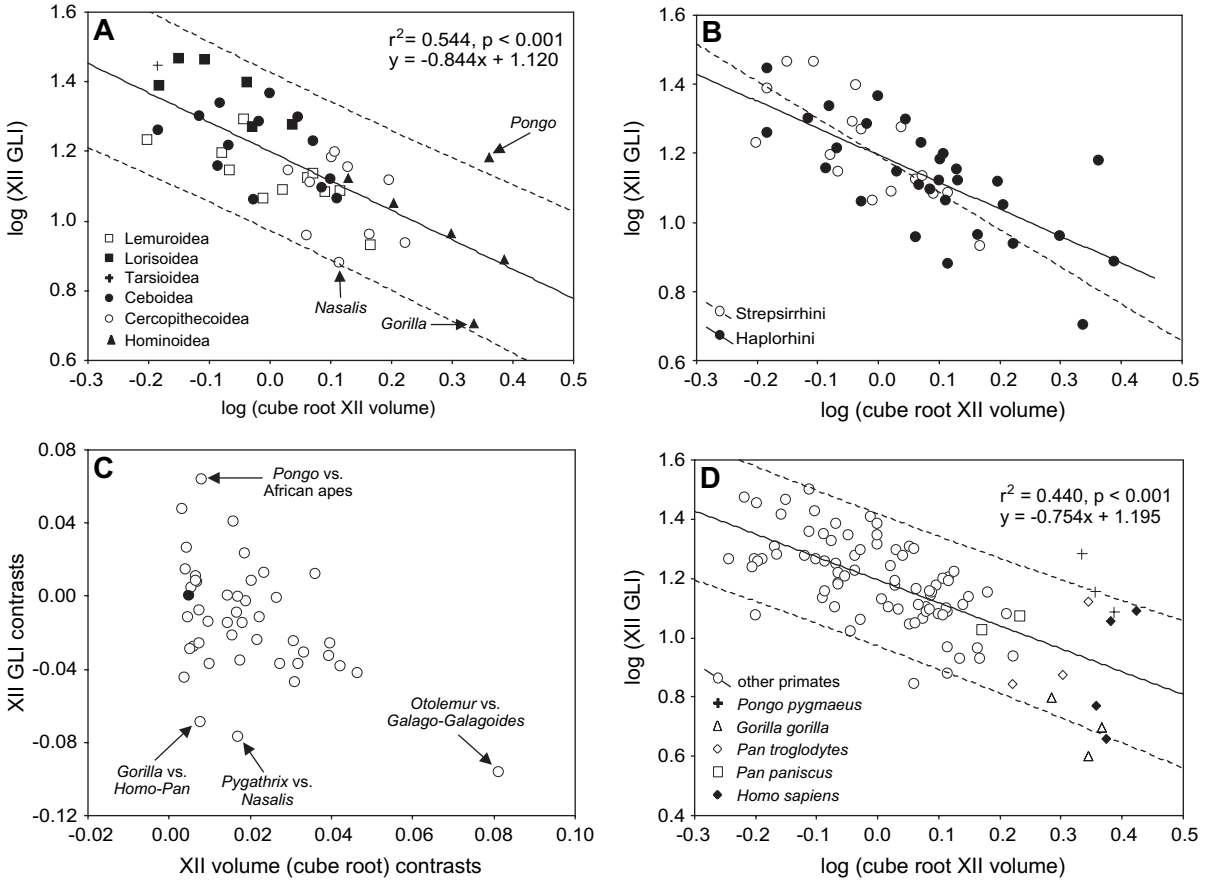

Fig. 12. Scaling analysis of XII GLI versus cube root XII volume in primates. (a) A least-squares regression line is fit to the entire primate sample with 95% prediction intervals shown. (b) Separate least-squares regression lines are fit through the strepsirrhines and haplorhines. (c) Independent contrasts showing the strepsirrhine-haplorhine contrast (black dot) and indicating the other contrasts that were significant outliers from the least-squares regression of all ICs. (d) The least-squares regression line and associated 95% prediction intervals were calculated from non-human haplorhine individuals. Human data points are plotted with respect to the prediction line.

1992; Sendtner et al., 2000; Banks and Noakes, 2002). In particular, it has been observed that motoneuron survival is dramatically diminished when skeletal muscle is destroyed by a cre/loxP-mediated strategy (Grieshammer et al., 1998) or limb bud removal during embryonic development (Oppenheim, 1985). Thus, the high number of neurotrophic factors that mediate motoneuron proliferation and survival indicates a complex interaction among these various molecular cues. Therefore, in considering the causes of interspecific variation in the size of motor nuclei, it is important to recognize that developing motoneuron pools respond to the combined influence of activity-independent growth cues in addition to activity-dependent epigenetic regulation of motoneuron survival mediated by interactions with presynaptic inputs, postsynaptic target skeletal muscles, and other components of the extracellular matrix.

As a proximate mechanism underlying the observed close correlation among the orofacial motor nuclei, diffusible growth factors that act across the medulla may stimulate similar levels of progenitor proliferation and cell rescue from apoptosis in several different motor nuclei during development. It has been shown, for instance, that

compared to control littermates, transgenic mice that over-express insulin-like growth factor-I display increased total medulla volume concomitant with larger volumes and lower neuron packing densities evident in several cranial motor nuclei (Dentremont et al., 1999).

Overall, GLIs of all orofacial motor nuclei were observed to be significantly negatively correlated with nucleus volumes, indicating increases in nucleus size are matched by decreases in the relative tissue volume occupied by cell somata. This implies an increase in the relative space occupied by elements such as dendrites, axons, and synapses. Grade shifts between strepsirrhines and haplorhines were not detected in the scaling of GLI on nucleus volume for any of the orofacial motor nuclei. Thus, it appears that the neuropil space in these nuclei is determined predominantly by allometric scaling and not phylogenetic specializations of these taxa. The scaling pattern of neuropil space in these nuclei may be explained by the activity of growth factors, such as NGF, which can induce sprouting of peripheral dendritic branches (Dityatev et al., 1995). Thus, some of the same growth processes that determine final neuron number may also influence enhanced dendritic sprouting and greater neuropil space between neurons, explaining the correlation between these two variables.

Insofar as increased neuropil is associated with relatively more extensive dendritic arbors on each motoneuron, it is important to note how these alterations affect neuronal processing capacity. Since the geometry of a motoneuron's dendritic tree influences how synaptic inputs at various sites on the arbor will be integrated at the axon hillock (Barrett, 1975), neurons with more elaborate arborization are more sensitive to variations in membrane resistance and more able to modulate dynamically the size and shape of the effective dendritic field (Korogod et al., 2000). Therefore, although it is impossible to know precise characteristics of dendritic geometry from the simple measurement of neuropil used in this study, increases in neuropil space at larger nucleus volumes might entail significant changes to the computational properties of motoneurons.

Size and microstructure of Vmo in relation to diet

We found that the scaling of Vmo volume and GLI did not differ between strepsirrhines and haplorhines. It has been claimed that progressive fusion of the mandibular symphysis in the evolution of stem anthropoids may have been related to the consumption of tougher diets that require relative increases in balancing-side jaw muscle force recruitment, greater repetitive loading of the mandible, and more dorsoventral shear (Ravosa, 1999). However, any such phylogenetic variation in jaw muscle recruitment and rhythmic loading does not appear to require relative enlargement of masticatory muscles in haplorhines. Cachel (1984) found that the muscles of mastication scale isometrically with body mass across both strepsirrhines and haplorhines. In addition, Ross (1995) did not find suborder differences in scaling exponents when temporalis muscle mass was regressed against skull length. Thus, scaling equality of Vmo volume and GLI between suborders might be explained by the fact that the peripheral target musculature, a major determinant of motoneuron population size, also does not evince phyletic variation in scaling relationships.

After controlling for phylogenetic bias (by calculating ICs) and adjustment for size (by calculating residuals), no significant correlations were found to support a functional interpretation of Vmo structure in relation to dietary toughness. Thus, our data suggest that extra-allometric neuroanatomical specializations of Vmo are not required to innervate the muscles of mastication in primates that consume highly fibrous diets. This result may reflect a lack of diet-related variation in either the target muscle fiber population or the density of innervation. Our data do not permit distinction between these alternatives. Nonetheless, our findings are consistent with the idea that the various skeletal biomechanical correlates of folivory, such as more anteriorly placed masticatory muscles, shortening of the jaw, and elevation of the mandibular condyle above the occlusal plane, may be sufficient in and of themselves to confer the masticatory efficiency and bite force to

the cheek teeth required to process tough foods (Herring and Herring, 1974; Hylander, 1979; Spencer, 1998).

Size and microstructure of VII in relation to social communication

Although we did not find a correlation between relative VII volume or GLI and social group size, significant phylogenetic differences in the scaling of VII volume were revealed. Of note, VII volume scaled against medulla volume with a significantly steeper slope in haplorhines than in strepsirrhines. In addition, the volume of VII in hominids was significantly greater than predicted based on the nonhominid haplorhine regression.

A possible explanation for this pattern of results might be that phylogenetic variation in cranial motor nuclei reflects only major changes to afferent systems and/or innervation of target musculature that occur at the base of adaptive radiations. In contrast, the social organization of primate species (with the exception of cercopithecoids) displays a striking amount of variation among congeners in response to ecological pressures (Di Fiore and Rendall, 1994). If this is the case, then any index of sociality, such as social group size, will tend to reflect recent ecological conditions, whereas neuromuscular adaptations will tend to reflect more ancient derived traits. Hence, the fact that VII structure was uncorrelated with social group size may be because these variables reflect adaptation to socioecological pressures at different evolutionary time scales. The apparent tendency for VII volume to vary primarily at higher taxonomic levels can be formally evaluated by examination of the correlation between ICs and node depth. However, a correlation does not exist between node depth and ICs for the volume of VII or any other orofacial motor nucleus, suggesting that if such a pattern is present, it is weak and does not consistently characterize branching points on the tree.

Nonetheless, most of the phylogenetic variance in the neuromuscular system controlling facial expression appears to represent character state transformations at the base of adaptive radiations. There are several significant differences between primate suborders in the configuration of the facial muscles of expression. The mimetic component of the facial musculature is not as highly differentiated in strepsirrhines as compared to anthropoids (Huber, 1931). In strepsirrhines, the facial musculature is specialized for the reception of auditory, olfactory, and tactile information that is relevant in a nocturnal environment. Several muscle bundles attach onto the external ear to enable mobility for sound localization and muscles in the region of the snout are well differentiated in association with specializations for olfactory and tactile sensation involving movements of the moist rhinarium and tactile vibrissae. In many ways, the facial muscles of tarsiers resemble the strepsirrhine condition (Huber, 1931).

Compared to strepsirrhines, the frontalis of anthropoids is more developed and is recruited in gestures involving raising of the forehead and eyebrows. In addition, the rhinarium, philtrum, and frenulum are absent, thereby permitting the development of an orbicularis oris that completely encircles the mouth (Huber, 1931), enabling a greater range of movement of the lips to generate a diverse range of signals (van Hooff, 1962; Chevalier-Skolnikoff, 1973). Compared to monkeys, the face of great apes and humans is characterized by reduction of ear, scalp, and forehead muscles, concomitant with increased differentiation of the muscles of the midfacial region to subserve more complex configuration of the lips for feeding, vocalizing, and facial displays (Huber, 1931, 1933; Andrew, 1963, 1965). Moreover, great apes and humans have relatively well-developed corrugator supercilii to draw the eyebrow downward and medially. In light of these data, we speculate that allometric departures of VII volume in haplorhines and hominids may be an epigenetic result of anatomic changes of peripheral musculature in these lineages. This modification of target musculature, in turn, might provide muscle-derived neurotrophic support and spare relatively more developing motoneurons from programmed cell death. Indeed, species mean VII volume is significantly correlated with stereologic estimates of VII neuron number in primates (Sherwood, 2003) ($r = 0.780$, $p = 0.001$, $n = 15$).

Of relevance, phylogenetic specializations of the orofacial representation in primary motor cortex (Brodmann's area 4) of primates have also been described. Tract-tracing and axon degeneration studies have revealed direct cortico-motoneuron innervation in VII of several anthropoid species (Walberg, 1957; Kuypers, 1958b, 1958c, 1967; Jenny and Saper, 1987; Sokoloff, 1989; Sokoloff and Deacon, 1990; Morecraft et al., 2001; Jürgens and Alipour, 2002). Comparative anatomic studies of corticospinal projections in mammals suggest that enhanced dexterity is correlated with elaboration of such direct cortico-motoneuron connections (Heffner and Masterton, 1975, 1983). In contrast, in non-anthropoid mammalian species, axonal projections from primary motor cortex terminate in the parvocellular reticular formation (e.g., Kuypers, 1958a; Sokoloff and Deacon, 1990; Alipour et al., 1997, 2002; Jürgens and Alipour, 2002) and have only indirect polysynaptic access to VII motoneurons (Travers and Norgren, 1983; Fay and Norgren, 1997; Travers and Rinaman, 2002). Also of note, compared to Old World monkeys, the orofacial representation of primary motor cortex in hominids is characterized by increased thickness of superficial cortical layers, decreased neuron packing density, increased proportions of neurofilament protein-containing neurons, and relatively greater numbers of transcolumnar inhibitory interneuron subtypes (Sherwood et al., 2003, 2004a, 2004b). While some of these microstructural features are certainly general differences in cortical organization attributable to network scaling at larger brain size (e.g., thickness of superficial cortical layers and neuron density), phylogenetic differences in the distribution of neuron subtypes have not yet been reliably quantified across a wide range of species and cortical areas. Therefore, the extent to which chemoarchitectural reorganization in the orofacial representation of primary motor cortex might reflect particular specializations for motor control versus general scaling trends is not yet clear.

Taken together, these neuroanatomic specializations for facial muscle mobility and control may have been necessary to subserve enhanced social communication skills involved in the adaptive radiations of anthropoids (van Hooff, 1962; Preuschoft and van Hooff, 1995) and hominids (Potts, 2004). For example, the degree to which the mouth is opened to display the teeth is highly variable in threat expressions of macaques, depending on the intensity of the signal (Maestripieri, 1997). These types of fine signal gradations allow for the communication of highly nuanced information and for the dynamic flexibility needed in negotiating complex social interactions, such as alliance formation, that are typical of these species (Cheney et al., 1987; Byrne and Whiten, 1988).

Evolution of speech abilities in humans

It has been hypothesized that the human tongue may receive greater density of innervation for fine motor control of speech articulation (Kay et al., 1998; Fitch, 2000). Although we were unable to obtain data on tongue mass from the specimens included in this study to directly examine relative innervation densities, our findings nonetheless suggest that the human hypoglossal motor system does not significantly differ from that of other primates. Considerable overlap was observed in the volume of XII among individual specimens of human, gorilla, and orang-utan. In addition, results from our comparative stereologic analysis of XII neuron numbers indicate even more extensive overlap in the distribution of XII neuron numbers among humans and great apes (Sherwood, 2003). When the observed volumes of XII in the human sample were compared to their predicted values based on the nonhuman haplorhine regression, these values fell above the line but did not exceed the 95% prediction intervals. However, data from orang-utan individuals had considerably larger residuals and observed values were above the prediction intervals. Therefore, XII enlargement does not appear to be exclusively associated with speech in humans. Grey Level Index values in humans, furthermore, did not differ from allometric expectations.

The neural mechanisms underlying human language have often been characterized as elaborations of pre-existing circuits in nonhuman primates (Deacon, 1997; Gannon et al., 1998; MacNeilage, 1998). In our analysis, the volume and microstructure of human orofacial motor

nuclei did not differ significantly from allometric expectations. In this regard, our results suggest that human linguistic abilities are built upon cytoarchitecturally unspecialized cranial nerve motor nuclei and do not require enhancement of fine motor control of orofacial muscles. It is interesting that lateral-projection videofluorography studies indicate that movements of the tongue surface in human speech do not occur outside the domain of movement observed for feeding in macaques and humans (Hiiemae, 2000; Hiiemae et al., 2002). In sum, these data support the hypothesis proposed by MacNeilage (1998) that the motor patterns of human speech are similar in form to oscillating visuofacial signals of nonhuman primates (e.g., lip smacks, tongue smacks, and teeth chatters) and may exploit conserved central pattern generators and motoneuron pool organization.

Although apes use many of the segmental phonetic elements found in human speech in their normal vocalizations (Hauser, 1996; Lieberman, 2002), their calls are closely linked to emotional states and they lack the capacity to execute the appropriate sequence of orofacial movements necessary to generate a series of speech phonemes (Marler and Tenaza, 1977). Clinical evidence indicates that higher order brain regions that subserve human speech, such as the inferior frontal cortex (i.e., Broca's area), basal ganglia, and cerebellum are also implicated in generating sequences of nonlinguistic orofacial and manual movements (Lieberman, 1991; Kimura, 1993; Leiner et al., 1993; Middleton and Strick, 1994). Broca's aphasics have severely impaired speech although they are unaffected in their ability to control the amplitude and placement of tongue, lips, and larynx movements in isolation as manifest by the preservation of formant frequency patterns that specify vowels in these patients (Kent and Rosenbeck, 1983; Ryalls, 1986; Baum et al., 1990). Patients with Parkinson's disease, which affects circuits of the basal ganglia, exhibit specific deficits in the production of syntactic structure in addition to more generalized motor impairment (Lieberman et al., 1992; Pickett et al., 1998). In this context, it is interesting that individuals who suffer from verbal and orofacial dyspraxia caused by mutation in the FOXP2 gene exhibit functional under-activation and morphological abnormalities of the inferior frontal cortex and basal ganglia (Belton et al., 2003; Liégeois et al., 2003). Moreover, the FOXP2 gene appears to have been the target of directional selection during human evolution (Enard et al., 2002). Findings from neuroimaging studies implicate the dentate nucleus and lateral cerebellar hemispheres in language processing and other non-motor cognitive tasks (Leiner et al., 1993; Ackermann et al., 1998; Schlosser et al., 1998) and cerebellar lesions have been noted to result in speech apraxia and ataxic dysarthria (Marien et al., 2001). Overall, these data suggest that the evolution of human speech required, in part, reorganization of higher-order brain areas involved in programming complex sequenced motor output and that provide descending innervation to orofacial motoneurons. The primary orofacial motoneuron pools themselves, however, appear to be evolutionarily conserved.

Other species-specific departures from allometric predictions

Several taxa were observed to be outliers in our scaling analyses. We are reluctant to offer ad hoc scenarios to explain species-specific allometric departures in cases where samples sizes are small ($n = 1$). Intraspecific variation in brain structure composition can be quite substantial, so the confound of sampling error must be considered a significant limitation to interpretation of outliers that are based on small intraspecific sample sizes (Sherwood et al., 2004c). Therefore, we will restrict our discussion only to species which were represented by at least two individuals. On this basis, Vmo was found to be relatively enlarged in *Macaca mulatta* and reduced in *Pan paniscus*, VII was relatively enlarged in *Otolemur crassicaudatus* and *Tarsius syrichta*, and XII was enlarged in *Pongo pygmaeus*. Departures from allometric expectations of GLI, furthermore, may indicate connectional specializations beyond basic scaling and growth patterns required for functional equivalence. *Pongo pygmaeus* had a greater GLI

than expected for all three orofacial motor nuclei and *Gorilla gorilla* had a lower GLI than predicted for its XII.

Some of these allometric departures make sense in the context of species-specific orofacial adaptations while others are difficult to reconcile with what is currently known about peripheral anatomy and behavior. If extra-allometric changes in nucleus volume are a reflection of the capacity of the brain to produce fine motor output to target muscles, then the finding that bonobos have a relatively small Vmo is difficult to square with the form and function of their masticatory system. Bonobos are similar to gorillas in relying more on terrestrial herbaceous vegetation than common chimpanzees (Malenkey and Wrangham, 1994), an ecological adaptation that is paralleled by cranial (Cramer, 1977) and dental (Kinzey, 1984; McCollum and McGrew, in press) differences. Increased terrestrial herbaceous vegetation in the diet requires greater chewing force and more daily chewing cycles (Taylor, 2002). Therefore, if a relationship exists between Vmo volume and masticatory muscle size, it would be reasonable to expect a correlated increase in the size of Vmo rather than the observed decrease.

Although *Tarsius* and *Otolemur* are nocturnal prosimians and do not rely substantially on visual communication in their social exchanges (Zeller, 1987), the enlargement of VII observed in these species may be associated with specializations of the superficial facial muscles for other purposes. There is evidence that the muscles of the pinna in *Otolemur crassicaudatus* possess a large number of fascicles per muscle, suggesting a role for VII enlargement in external ear movements for sound localization (Burrows and Smith, 2003). In tarsiers, the orbicularis oculi and depressor palpebrae inferioris are specialized in their fiber structure to protect the exceptionally large eyeball (Huber, 1931). In addition, highly differentiated muscles are found around the mobile ear cartilage and in the nasolabial region to move the prominent tactile vibrissae. Finally, it is possible that relative enlargement of XII in orang-utans is associated with their impressive capacity to manipulate tools with their lips, teeth, and tongue (van Schaik et al., 1996; O'Malley and McGrew, 2000), although if this is the case, then it is unclear why VII of orang-utans is not also enlarged.

At present it is impossible to determine the specific connectivity that accounts for apparent specializations of GLI and so it is difficult to offer an interpretation. In particular, if relative neuropil volume has any relation whatsoever to motor dexterity, then it is difficult to explain the fact that orang-utans have relatively less neuropil in all orofacial motor nuclei considering their skillful abilities to manipulate objects with their lips and tongue as mentioned above.

Finally, it is worth noting that our analysis considered only volume and GLI within whole nuclei. Qualitative observation, however, indicates that there is phylogenetic variation with respect to the differentiation of subdivisions within each motor nucleus (Fig. 2). Hence, it is possible that more subtle aspects of microstructural organization such as dendritic morphology, differentiation of subnuclei, or the distribution of neuronal subtypes may reveal more significant interspecific differences. Indeed, each of the orofacial motor nuclei contains a musculotopic arrangement of neurons organized into subnuclei that innervate specific subsets of muscles and available evidence indicates notable variation among mammalian species in the relative sizes of these subnuclei (e.g., Courville, 1966; Komiyama et al., 1984; Friauf and Herbert, 1985; Semba and Egger, 1986; Sokoloff, 1989; Welt and Abbs, 1990). It is possible, therefore, that variation in the organization of subdivisions within orofacial motor nuclei underlies more precise patterns of phylogenetic and functional diversity not revealed in our study. For example, closer examination of the lateral subdivision of VII, which innervates muscles of the mouth, may reveal correlated neuroanatomical adaptations for social complexity. Unfortunately, there are not distinct cytoarchitectural boundaries between subdivisions of many motor nuclei that allow for reliable segmentation based on Nissl-stained materials (Fig. 2).

Conclusions

The results of this study reveal a mosaic of conservative and derived traits in the orofacial

motor nuclei of primates. In general, the volume and neuropil space in these nuclei were closely correlated with overall size variables, a finding that emphasizes the important role of developmental constraint in determination of the volume and cytoarchitecture of these brainstem nuclei. We tested several hypotheses relating the structure of the orofacial motor nuclei to functional and phylogenetic specializations. For the most part, however, variation in these motor nuclei was not clearly associated with such adaptations. After controlling for phylogenetic bias, there was no apparent relationship between the neuroanatomic organization of these nuclei with socioecological variables, such as social group size or the percentage of leaves in the diet. In addition, despite phylogenetic variation in the masticatory system as evident by mandibular symphysis fusion in anthropoids, the scaling of Vmo did not differ between primate suborders. Our analyses also did not find evidence to support the hypothesis that the human hypoglossal motor system is uniquely reorganized to facilitate articulate speech. In fact, orang-utans displayed relatively larger hypoglossal nucleus volumes than humans. Nonetheless, we found several instances where taxa exhibited significant departures from conservative allometric scaling patterns. A grade shift was observed in the scaling of XII volume such that the strepsirrhine regression line had a higher elevation than the haplorhine line. In addition, VII volume scaled with a steeper slope in haplorhines compared to strepsirrhines, perhaps reflecting a difference between these phylogenetic groups in the developmental mechanisms that regulate VII motoneuron proliferation and subsequent elimination. Hominids, furthermore, were found to have significantly larger VII volumes than predicted for nonhominid haplorhines of their medulla volume. Taken together, these phylogenetic specializations of VII may be related to variation in facial muscle differentiation and increased descending inputs from neocortical areas. These modifications may constitute a neuroanatomic substrate for the evolution of fine motor control to the facial muscles of expression in these taxa in association with increased emphasis on gestural modes of communication utilizing the visual channel.

Acknowledgements

We thank Drs. J.K. Rilling, C.J. Terranova, C.J. Vinyard, S.C. McFarlin, and the anonymous reviewers for helpful suggestions that improved this manuscript. We thank Dr. J.M. Erwin for constant interest and support. Dr. C.E. MacLeod generously shared shrinkage correction factor data. This work was supported by the Leakey Foundation, the Wenner-Gren Foundation for Anthropological Research, NSF BCS-0121286, NSF SBE-SBR-9617262, NSF IBN-9905402, NSF DBI-9602234 (to NYCEP), and the Mount Sinai School of Medicine. Part of this work was supported by a grant to K.Z. (Human Brain Project/Neuroinformatics research funded by the National Institute of Biomedical Imaging and Bioengineering, the National Institute of Neurological Disorders and Stroke, and the National Institute of Mental Health). P.R.H. is the Regenstreif Professor of Neuroscience.

References

Ackermann, H., Wildgruber, D., Daum, I., Grodd, W., 1998. Does the cerebellum contribute to cognitive aspects of speech production? A functional magnetic resonance imaging (fMRI) study in humans. Neurosci. Lett. 247, 187–190.

Adolphs, R., Tranel, D., Damasio, H., Damasio, A.R., 1995. Fear and the human amygdala. J. Neurosci. 15, 5879–5891.

Alipour, M., Chen, Y., Jürgens, U., 1997. Anterograde projections of the cortical tongue area of the tree shrew (*Tupaia belangeri*). J. Hirnforsch. 38, 405–423.

Alipour, M., Chen, Y., Jürgens, U., 2002. Anterograde projections of the motorcortical tongue area in the saddleback tamarin (*Saguinus fuscicollis*). Brain Behav. Evol. 60, 101–116.

Allman, J.M., 1999. Evolving Brains. Scientific American Library, New York.

Andrew, R.J., 1963. Evolution of facial expression. Science 142, 1034–1041.

Andrew, R.J., 1965. The origins of facial expression. Sci. Am. 213, 88–94.

Ariëns Kappers, C.U., Huber, G.C., Crosby, E.C., 1936. The Comparative Anatomy of the Nervous System of Vertebrates, Including Man, vol. I. Macmillan Company, New York.

Banks, G.B., Noakes, P.G., 2002. Elucidating the molecular mechanisms that underlie the target control of motoneuron death. Int. J. Dev. Biol. 46, 551–558.

Baron, G., Frahm, H.D., Stephan, H., 1988. Comparison of brain structure volumes in Insectivora and Primates. VIII. Vestibular complex. J. Hirnforsch. 5, 509–523.

Baron, G., Stephan, H., Frahm, H.D., 1990. Comparison of brain structure volumes in Insectivora and Primates. IX. Trigeminal complex. J. Hirnforsch. 31, 193–200.

Baron, G., Stephan, H., Frahm, H.D., 1996. Comparative Neurobiology in Chiroptera. Birkhäuser Verlag, Basel.

Barrett, J.N., 1975. Motoneuron dendrites: role in synaptic integration. Fed. Proc. 34, 1398–1407.

Barton, R.A., 1999. The evolutionary ecology of the primate brain. In: Lee, P.C. (Ed.), Comparative Primate Socioecology. Cambridge University Press, Cambridge, pp. 167–203.

Baum, S.R., Blumstein, S.E., Naeser, M.A., Palumbo, C.L., 1990. Temporal dimensions of consonant and vowel production: an acoustic and CT scan analysis of aphasic speech. Brain Lang. 39, 33–56.

Belton, E., Salmond, C.H., Watkins, K.E., Vargha-Khadem, F., Gadian, D.G., 2003. Bilateral brain abnormalities associated with dominantly inherited verbal and orofacial dyspraxia. Hum. Brain Mapp. 18, 194–200.

Blomberg, S.P., Garland, T., Ives, A.R., 2003. Testing for phylogenetic signal in comparative data: behavioral traits are more labile. Evolution 57, 717–745.

Bruce, C., Desimone, R., Gross, C.G., 1981. Visual properties of neurons in a polysensory area in superior temporal sulcus of the macaque. J. Neurophysiol. 46, 369–384.

Burrows, A.M., Smith, T.D., 2003. Muscles of facial expression in *Otolemur*, with a comparison to Lemuroidea. Anat. Rec. 274A, 827–836.

Byrne, R.W., Whiten, A., 1988. Machiavellian Intelligence: Social Expertise and the Evolution of Intellect in Monkeys, Apes, and Humans. Clarendon Press, Oxford.

Byrne, R.W., Whiten, A., 1992. Cognitive evolution in primates: evidence from tactical deception. Man 27, 609–627.

Cachel, S., 1984. Growth and allometry in primate masticatory muscles. Archs. Oral Biol. 29, 287–293.

Cameron, H.A., Hazel, T.G., McKay, R.D., 1998. Regulation of neurogenesis by growth factors and neurotransmitters. J. Neurobiol. 36, 287–306.

Cheney, D.L., Seyfarth, R.M., Smuts, B.B., Wrangham, R.W., 1987. The study of primate societies. In: Smuts, B.B., Cheney, D.L., Seyfarth, R.M., Wrangham, R.W., Strusaker, T.T. (Eds.), Primate Societies. University of Chicago, Chicago, pp. 1–8.

Chevalier-Skolnikoff, S., 1973. Facial expression of emotion in nonhuman primates. In: Ekman, P. (Ed.), Darwin and Facial Expression. Academic Press, New York, pp. 11–90.

Chevalier-Skolnikoff, S., 1982. A cognitive analysis of facial behavior in Old World monkeys, apes, and human beings. In: Snowdon, C.T., Brown, C.H., Petersen, M.R. (Eds.), Primate Communication. Cambridge University Press, Cambridge, pp. 303–368.

Courville, J., 1966. The nucleus of the facial nerve: the relation between cellular groups and peripheral branches of the facial nerve. Brian Res. 1, 338–354.

Cramer, D.L., 1977. Craniofacial morphology of *Pan paniscus*. Contrib. Primatol. 10, 1–64.

Crosby, E.C., Humphery, T., Lauer, E.W., 1962. Correlative Anatomy of the Nervous System. Macmillan, New York.

Dauvergne, C., Pinganaud, G., Buisseret, P., Buisseret-Delmas, C., Zerari-Mailly, F., 2001. Reticular premotor neurons projecting to both facial and hypoglossal nuclei receive trigeminal afferents in rats. Neurosci. Lett. 311, 109–112.

Deacon, T.W., 1990. Fallacies of progression in theories of brain-size evolution. Int. J. Primatol. 11, 193–235.

Deacon, T.W., 1997. The Symbolic Species: The Co-evolution of Language and the Brain. W.W. Norton & Company, Inc, New York.

Deaner, R.O., Barton, R.A., van Schaik, C.P., 2002. Primate brains and life histories: renewing the connection. In: Kappeler, P.M., Pereira, M.E. (Eds.), Primate Life Histories and Socioecology. University of Chicago Press, Chicago, pp. 233–265.

DeGusta, D., Glibert, W.H., Turner, S.P., 1999. Hypoglossal canal size and hominid speech. Proc. Natl. Acad. Sci. USA 96, 1800–1804.

Dentremont, K.D., Ye, P., D'Ercole, A.J., O'Kusky, J.R., 1999. Increased insulin-like growth factor-I (IGF-I) expression during early postnatal development differentially increases neuron number and growth in medullary nuclei of the mouse. Dev. Brain. Res. 114, 135–141.

Desimone, R., Albright, T.D., Gross, C.G., Bruce, C., 1984. Stimulus-selective properties of inferior temporal neurons in the macaque. J. Neurosci. 4, 2051–2062.

de Waal, F.B.M., 1982. Chimpanzee Politics. Jonathan Cape, London.

Di Fiore, A., Rendall, D., 1994. Evolution of social organization: a reappraisal for primates by using phylogenetic methods. Proc. Natl. Acad. Sci. USA 91, 9941–9945.

Dityatev, A.E., Chmykhova, N.M., Studer, L., Karamian, O.A., Kozhanov, V.M., Clamann, H.P., 1995. Comparison of the topology and growth rules of motoneuronal dendrites. J. Comp. Neurol. 363, 505–516.

Dunbar, R.I.M., 1992. Neocortex size as a constraint on group size in primates. J. Hum. Evol. 20, 469–493.

Dunbar, R.I.M., 1998. The social brain hypothesis. Evol. Anthropol. 6, 178–190.

Enard, W., Przeworski, M., Fisher, S.E., Lai, C.S., Wiebe, V., Kitano, T., Monaco, A.P., Pääbo, S., 2002. Molecular evolution of FOXP2, a gene involved in speech and language. Nature 418, 869–872.

Fay, R.A., Norgren, R., 1997. Identification of rat brainstem multisynaptic connections to the oral motor nuclei using pseudorabies virus. III. Lingual muscle motor systems. Brain Res. Rev. 25, 291–311.

Felsenstein, J., 1985. Phylogenies and the comparative method. Am. Nat. 125, 1–15.

Finlay, B.L., Darlington, R.B., 1995. Linked regularities in the development and evolution of mammalian brains. Science 268, 1578–1584.

Fitch, W.T., 2000. The evolution of speech: a comparative review. Trends Cogn. Sci. 4, 258–267.

Friauf, E., Herbert, H., 1985. Topographic organization of facial motoneurons to individual pinna muscles in rat (*Rattus rattus*) and bat (*Rousettus aegyptiacus*). J. Comp. Neurol. 240, 161–170.

Gallyas, F., 1971. A principle for silver staining of tissue elements by physical development. Acta Morphol. Acad. Sci. Hung. 19, 57–71.

Gannon, P.J., Holloway, R.L., Broadfield, D.C., Braun, A.R., 1998. Asymmetry of chimpanzee planum temporale: humanlike pattern of Wernicke's brain language area homolog. Science 279, 220–222.

Garland, T., Harvey, P.H., Ives, A.R., 1992. Procedures for the analysis of comparative data using phylogenetically independent contrasts. Syst. Biol. 41, 18–32.

Garland, T., Ives, A.R., 2000. Using the past to predict the present: confidence intervals for regression equations in phylogenetic comparative methods. Am. Nat. 155, 346–364.

Garland, T., Midford, P.E., Ives, A.R., 1999. An introduction to phylogenetically based statistical methods, with a new method confidence intervals on ancestral values. Am. Zool. 39, 374–388.

Glendenning, K.K., Masterton, R.B., 1998. Comparative morphometry of mammalian central auditory systems: variation in nuclei and form of the ascending system. Brain Behav. Evol. 51, 59–89.

Goodall, J., 1986. The Chimpanzees of Gombe. Harvard University Press, Cambridge.

Grieshammer, U., Lewandoski, M., Prevette, D., Oppenheim, R.W., Martin, G.R., 1998. Muscle-specific cell ablation conditional upon Cre-mediated DNA recombination in transgenic mice leads to massive spinal and cranial motoneuron loss. Dev. Biol. 197, 234–247.

Harvey, P.H., Krebs, J.R., 1990. Comparing brains. Science 249, 140–146.

Harvey, P.H., Pagel, M.D., 1991. The Comparative Method in Evolutionary Biology. Oxford University Press, Oxford.

Hasselmo, M.E., Rolls, E.T., Baylis, G.C., 1989. The role of expression and identity in the face-selective responses of neurons in the temporal visual cortex of the monkey. Behav. Brain Res. 32, 203–218.

Hauser, M.D., 1996. The Evolution of Communication. MIT Press, Cambridge.

Hauser, M.D., Schon Ybarra, M., 1994. The role of lip configuration in monkey vocalizations: experiments using xylocaine as a nerve block. Brain Lang. 46, 232–244.

Heffner, R., Masterton, B., 1975. Variation in form of the pyramidal tract and its relationship to digital dexterity. Brain Behav. Evol. 12, 161–200.

Heffner, R.S., Masterton, R.B., 1983. The role of the corticospinal tract in the evolution of human digital dexterity. Brain Behav. Evol. 23, 165–183.

Herring, S.W., Herring, S.E., 1974. The superficial masseter and gape in mammals. Am. Nat. 108, 561–576.

Hiiemae, K., 2000. The oro-facial complex in macaques: tongue and jaw movements in feeding. In: Whitehead, P.F., Jolly, C.J. (Eds.), Old World Monkeys. Cambridge University Press, Cambridge, pp. 214–236.

Hiiemae, K.M., Palmer, J.B., Medicis, S.W., Hegener, J., Jackson, B.S., Lieberman, D.E., 2002. Hyoid and tongue surface movements in speaking and eating. Arch. Oral Biol. 47, 11–27.

Holloway, R.L., Post, D.G., 1982. The relativity of relative brain measures and hominid mosaic evolution. In: Armstrong, E., Falk, D. (Eds.), Primate Brain Evolution: Methods and Concepts. Plenum Press, New York, pp. 57–76.

Huber, E., 1931. Evolution of Facial Musculature and Facial Expression. Johns Hopkins University Press, Baltimore.

Huber, E., 1933. The facial musculature and its innervation. In: Hartman, C.G., Straus Jr., W.L. (Eds.), The Anatomy of the Rhesus Monkey. Hafner, New York.

Hutcheon, J.M., Kirsch, J.A.W., Garland, T., 2002. A comparative analysis of brain size in relation to foraging ecology and phylogeny in the Chiroptera. Brain Behav. Evol. 60, 165–180.

Hylander, W.L., 1979. The functional significance of primate mandibular form. J. Morphol. 160, 223–240.

Hylander, W.L., Crompton, A.W., 1986. Jaw movements and patterns of mandibular bone strain during mastication in the monkey *Macaca fascicularis*. Arch. Oral Biol. 31, 841–848.

Hylander, W.L., Johnson, K.R., 1993. Modelling relative masseter force from surface electromyograms during mastication in non-human primates. Arch. Oral Biol. 38, 233–240.

Hylander, W.L., Johnson, K.R., 1994. Jaw muscle function and wishboning of the mandible during mastication in macaques and baboons. Am. J. Phys. Anthropol. 94, 523–547.

Hylander, W.L., Ravosa, M.J., Ross, C.F., Wall, C.E., Johnson, K.R., 2000. Symphyseal fusion and jaw-adductor muscle force: an EMG study. Am. J. Phys. Anthropol. 112, 469–492.

Jenny, A.B., Saper, C.B., 1987. Organization of the facial nucleus and corticofacial projection in the monkey: a reconsideration of the upper motor neuron facial palsy. Neurology 37, 930–939.

Jungers, W.L., Pokempner, A.A., Kay, R.F., Cartmill, M., 2003. Hypoglossal canal size in living hominoids and the evolution of human speech. Hum. Biol. 75, 473–484.

Jürgens, U., Alipour, M., 2002. A comparative study on the cortico-hypoglossal connections in primates, using biotin dextranamine. Neurosci. Lett. 328, 245–248.

Kanwisher, N., McDermott, J., Chun, M.M., 1997. The fusiform face area: a module in human extrastriate cortex specialized for face perception. J. Neurosci. 17, 4302–4311.

Kay, R.F., Cartmill, M., Balow, M., 1998. The hypoglossal canal and the origin of human vocal behavior. Proc. Natl. Acad. Sci. USA 95, 5417–5419.

Kent, R., Rosenbeck, J., 1983. Acoustic patterns of apraxia of speech. J. Speech Hear. Res. 26, 231–248.

Kimura, D., 1993. Neuromotor Mechanisms in Human Communication. Oxford University Press, New York.

Kinzey, W.G., 1984. The dentition of the pygmy chimpanzee, *Pan paniscus*. In: Susman, R.L. (Ed.), The Pygmy Chimpanzee: Evolutionary Biology and Behavior. Plenum Press, New York, pp. 65–88.

Komiyama, M., Shibata, H., Suzuki, T., 1984. Somatotopic representation of facial muscles within the facial nucleus of the mouse. A study using the retrograde horseradish peroxidase and cell degeneration techniques. Brain Behav. Evol. 24, 144–151.

Korogod, S.M., Kulagina, I.B., Horcholle-Bossavit, G., Gogan, P., Tyc-Dumont, S., 2000. Activity-dependent reconfiguration of the effective dendritic field of motoneurons. J. Comp. Neurol. 422, 18–34.

Kuypers, H.G.J.M., 1958a. An anatomical analysis of corticobulbar connections to the pons and lower brainstem in the cat. J. Anat. 92, 198–218.

Kuypers, H.G.J.M., 1958b. Corticobulbar connections to the pons and lower brainstem in man. Brain 81, 364–388.

Kuypers, H.G.J.M., 1958c. Some projections from the peri-central cortex to the pons and lower brainstem in monkey and chimpanzee. J. Comp. Neurol. 110, 221–251.

Kuypers, H.G.J.M., Lawrence, D.G., 1967. Cortical projections to the red nucleus and brain stem in the rhesus monkey. Brain Res. 4, 151–188.

Laitman, J.T., Heimbuch, R.C., Crelin, E.S., 1978. Developmental change in a basicranial line and its relationship to the upper respiratory system in living primates. Am. J. Anat. 152, 467–482.

Leiner, H.C., Leiner, A.L., Dow, R.S., 1993. Cognitive and language functions of the human cerebellum. Trends Neurosci. 16, 444–447.

Leonard, C.M., Rolls, E.T., Wilson, F.A., Baylis, G.C., 1985. Neurons in the amygdala of the monkey with responses selective for faces. Behav. Brain Res. 15, 159–176.

Li, Y.Q., Takada, M., Kaneko, T., Mizuno, N., 1997. Distribution of GABAergic and glycinergic premotor neurons projecting to the facial and hypoglossal nuclei in the rat. J. Comp. Neurol. 378, 283–294.

Li, Y.Q., Takada, M., Mizuno, N., 1993a. Premotor neurons projecting simultaneously to two orofacial motor nuclei by sending their branched axons. A study with a fluorescent retrograde double-labeling technique in the rat. Neurosci. Lett. 152, 29–32.

Li, Y.-Q., Takada, M., Mizuno, N., 1993b. Identification of premotor interneurons which project bilaterally to the trigeminal motor, facial or hypoglossal nuclei: a flourescent retrograde double-labeling study in the rat. Brain Res. 611, 160–164.

Lieberman, P., 1984. The Biology and Evolution of Language. Harvard University Press, Cambridge.

Lieberman, P., 1991. Uniquely Human. Harvard University Press, Cambridge.

Lieberman, P., 2002. On the nature and evolution of the neural bases of human language. Yearb. Phys. Anthropol. 45, 35–62.

Lieberman, P., Kako, E., Friedman, J., Tajchman, G., Feldman, L.S., Jiminez, E.B., 1992. Speech production, syntax comprehension, and cognitive deficits in Parkinson's disease. Brain Lang. 43, 169–189.

Liégeois, F., Baldeweg, T., Connelly, A., Gadian, D.G., Mishkin, M., Vargha-Khadem, F., 2003. Language fMRI abnormalities associated with FOXP2 gene mutation. Nat. Neurosci. 6, 1230–1237.

Lucas, P.W., Turner, I.M., Dominy, N.J., Yamashita, N., 2000. Mechanical defenses to herbivory. Ann. Bot. 86, 913–920.

MacLeod, C.E., 2000. The cerebellum and its part in the evolution of the hominoid brain. Ph.D. Dissertation, Simon Fraser University.

MacNeilage, P.F., 1998. The frame/content theory of evolution of speech production. Behav. Brain Sci. 21, 499–511.

Maestripieri, D., 1997. Gestural communication in macaques: usage and meaning of nonvocal signals. Evol. Commun. 1, 193–222.

Malenkey, R.K., Wrangham, R.W., 1994. A quantitative comparison of terrestrial herbacious food consumption by *Pan paniscus* in the Lomako Forest, Zaire, and *Pan troglodytes* in the Kibale Forest, Uganda. Am. J. Primatol. 32, 1–12.

Marien, P., Engelborghs, S., Fabbro, F., De Deyn, P.P., 2001. The lateralized linguistic cerebellum: a review and a new hypothesis. Brain Lang. 79, 580–600.

Marler, P., Tenaza, R., 1977. Signalling behavior of apes with special reference to vocalizations. In: Sebeok, T.E. (Ed.), How Animals Communicate. Indiana University Press, Bloomington, pp. 965–1033.

Martin, R.D., 1990. Primate Origins and Evolution. Princeton University Press, Princeton.

Matano, S., 1986. A volumetric comparison of the vestibular nuclei in primates. Folia Primatol. 47, 189–203.

McCollum, M.A., McGrew, W.C. Incisor attrition and size in bonobos: dietary implications for the evolution of sociality. Am. J. Phys. Anthropol., in press.

Merker, B., 1983. Silver staining of cell bodies by means of physical development. J. Neurosci. Methods 9, 235–241.

Middleton, F.A., Strick, P.L., 1994. Anatomical evidence for cerebellar and basal ganglia involvement in higher cognitive function. Science 266, 458–461.

Morecraft, R.J., Louie, J.L., Herrick, J.L., Stilwell-Morecraft, K.S., 2001. Cortical innervation of the facial nucleus in the non-human primate: a new interpretation of the effects of stroke and related subtotal brain trauma on the muscles of facial expression. Brain 124, 176–208.

Nara, T., Goto, N., Hamano, S., 1991. Development of the human dorsal nucleus of vagus nerve: a morphometric study. J. Auton. Nerv. Syst. 33, 267–275.

Nara, T., Goto, N., Nozaki, H., Maekawa, K., 1989. Development of the human facial nucleus: a morphometric study. No. To. Hattatsu 21, 453–459.

Nishimura, T., Mikami, A., Suzuki, J., Matsuzawa, T., 2003. Descent of the larynx in chimpanzee infants. Proc. Natl. Acad. Sci. USA 100, 6930–6933.

O'Malley, R.C., McGrew, W.C., 2000. Oral tool use by captive orangutans (*Pongo pygmaeus*). Folia Primatol. 71, 334–341.

Oppenheim, R.W., 1985. Naturally occurring cell death during neuronal development. Trends Neurosci. 8, 487–493.

Pannese, E., 1994. Neurocytology: Fine Structure of Neurons, Nerve Processes, and Neuroglial Cells. Thieme Medical Publisher, Inc., New York.

Perrett, D.I., Rolls, E.T., Caan, W., 1982. Visual neurones responsive to faces in the monkey temporal cortex. Exp. Brain Res. 47, 329–342.

Peters, M., Ploog, D., 1973. Communication among primates. Annu. Rev. Physiol. 35, 221–242.

Pickett, E.R., Kuniholm, E., Protopapas, A., Friedman, J., Lieberman, P., 1998. Selective speech motor, syntax and cognitive deficits associated with bilateral damage to the putamen and the head of the caudate nucleus: a case study. Neuropsychologia 36, 173–188.

Popratiloff, A.S., Streppel, M., Gruart, A., Guntinas-Lichius, O., Angelov, D.N., Stennert, E., Delgado-Garcia, J.M., Neiss, W.F., 2001. Hypoglossal and reticular interneurons involved in oro-facial coordination in the rat. J. Comp. Neurol. 433, 364–379.

Potts, R., 2004. Paleoenvironmental basis of cognitive evolution in great apes. Am. J. Primatol. 62, 209–228.

Preuschoft, S., van Hooff, J.A., 1995. Homologizing primate facial displays: a critical review of methods. Folia Primatol. 65, 121–137.

Preuss, T.M., Goldman-Rakic, P.S., 1991. Architectonics of the parietal and temporal association cortex in the strepsirhine primate *Galago* compared to the anthropoid primate *Macaca*. J. Comp. Neurol. 310, 475–506.

Puce, A., Allison, T., Asgari, M., Gore, J.C., McCarthy, G., 1996. Differential sensitivity of human visual cortex to faces, letterstrings, and textures: a functional magnetic resonance imaging study. J. Neurosci. 16, 5205–5215.

Purvis, A., 1995. A composite estimate of primate phylogeny. Philos. Trans. R. Soc. Lond. B Biol. Sci. 348, 405–421.

Purvis, A., Rambaut, A., 1995. Comparative analysis by independent contrasts (CAIC): an Apple Macintosh application for analysing comparative data. Comput. Appl. Biosci. 11, 247–251.

Purvis, A., Webster, A.J., 1999. Phylogenetically independent comparisons and primate phylogeny. In: Lee, P.C. (Ed.), Comparative Primate Socioecology. Cambridge University Press, Cambridge, pp. 44–68.

Ravosa, M.J., 1990. Functional assessment of subfamily variation in maxillomandibular morphology among Old World monkeys. Am. J. Phys. Anthropol. 82, 199–212.

Ravosa, M.J., 1999. Anthropoid origins and the modern symphysis. Folia Primatol. 70, 65–78.

Rider, T.W., Calvard, S., 1978. Picture thresholding using an iterative selection method. IEEE Trans. Syst. Man Cybern. 8, 630–632.

Rilling, J.K., Insel, T.R., 1999. The primate neocortex in comparative perspective using magnetic resonance imaging. J. Hum. Evol. 37, 191–223.

Rilling, J.K., Seligman, R.A., 2002. A quantitative morphometric comparative analysis of the primate temporal lobe. J. Hum. Evol. 42, 505–533.

Rolls, E.T., 1984. Neurons in the cortex of the temporal lobe and in the amygdala of the monkey with responses selective for faces. Hum. Neurobiol. 3, 209–222.

Ross, C., 1995. Muscular and osseous anatomy of the primate anterior temporal fossa and the functions of the postorbital septum. Am. J. Phys. Anthropol. 98, 275–306.

Ross, C., Jones, K.E., 1999. Socioecology and the evolution of primate reproductive rates. In: Lee, P.C. (Ed.), Comparative Primate Socioecology. Cambridge University Press, Cambridge, pp. 73–110.

Ross, C.F., 2000. Into the light: the origin of Anthropoidea. Annu. Rev. Anthropol. 29, 147–194.

Ryalls, J.H., 1986. An acoustic study of vowel production in aphasia. Brain Lang. 29, 48–67.

Schlaug, G., Armstrong, E., Schleicher, A., Zilles, K., 1993. Layer V pyramidal cells in the adult human cingulate cortex: a quantitative Golgi study. Anat. Embryol. 187, 515–522.

Schleicher, A., Zilles, K., 1990. A quantitative approach to cytoarchitectonics: analysis of structural inhomogeneities in nervous tissue using an image analyzer. J. Microsc. 157, 367–381.

Schlosser, R., Hutchinson, M., Joseffer, S., Rusinek, H., Saarimaki, A., Stevenson, J., Dewey, S.L., Brodie, J.D., 1998. Functional magnetic resonance imaging of human brain activity in a verbal fluency task. J. Neurol. Neurosurg. Psychiatry 64, 492–498.

Schultz, A., 1969. The Life of Primates. Weidenfeld & Nicholson, London.

Semba, K., Egger, M.D., 1986. The facial "motor" nerve of the rat: control of vibrissal movement and examination of motor and sensory components. J. Comp. Neurol. 247, 144–158.

Sendtner, M., Pei, G., Beck, M., Schweizer, U., Wiese, S., 2000. Developmental motoneuron cell death and neurotrophic factors. Cell Tissue Res. 301, 71–84.

Sherwood, C.C., 2003. Neural substrates of primate communication: a comparative histometric study of the orofacial motor system. Ph.D. Dissertation, Columbia University.

Sherwood, C.C., Holloway, R.L., Erwin, J.M., Hof, P.R., 2004a. Cortical orofacial motor representation in Old World monkeys, great apes, and humans. II. Stereologic analysis of chemoarchitecture. Brain Behav. Evol. 63, 82–106 (and erratum Brain Behav. Evol. (2005) 65, 71–72).

Sherwood, C.C., Holloway, R.L., Erwin, J.M., Schleicher, A., Zilles, K., Hof, P.R., 2004b. Cortical orofacial motor representation in Old World monkeys, great apes, and humans. I. Quantitative analysis of cytoarchitecture. Brain Behav. Evol. 63, 61–81.

Sherwood, C.C., Cranfield, M.R., Mehlman, P.T., Lilly, A.A., Garbe, J.A., Whittier, C.A., Nutter, F.B., Rein, T.R., Bruner, H.J., Holloway, R.L., Tang, C.Y., Naidich, T.P., Delman, B.N., Steklis, H.D., Erwin, J.M., Hof, P.R., 2004c. Brain structure variation in great apes, with attention to the mountain gorilla (*Gorilla beringei beringei*). Am. J. Primatol. 63, 149–164.

Sherwood, C.C., Holloway, R.L., Gannon, P.J., Semendeferi, K., Erwin, J.M., Zilles, K., Hof, P.R., 2003. Neuroanatomical basis of facial expression in monkeys, apes, and humans. Ann. NY Acad. Sci. 1000, 99–103.

Smith, R.J., 1993. Logarithmic transformation bias in allometry. Am. J. Phys. Anthropol. 90, 215–228.

Sohal, G.S., Hirano, S., Kumaresan, K., Ali, M.M., 1992. Influence of altered afferent input on the number of trochlear motor neurons during development. J. Neurobiol. 23, 10–16.

Sokoloff, A., Deacon, T.W., 1990. Direct projections from the face area of primary motor cortex to the facial nucleus in cynomolgus monkey but not in the cat or rat. Am. J. Phys. Anthropol. 81, 298.

Sokoloff, A.J., 1989. The organization of the hypoglossal nucleus: an experimental neuroanatomical investigation of hypoglossal-lingual and cortico-hypoglossal projections in *Macaca fascicularis* and other vertebrate species. Ph.D. Dissertation, Harvard University.

Spencer, M.A., 1998. Force production in the primate masticatory system: electromyographic tests of biomechanical hypotheses. J. Hum. Evol. 34, 25–54.

Stephan, H., Baron, G., Frahm, H.D., 1988. Comparative size of brains and brain components. In: Steklis, H.D., Erwin, J. (Eds.), Comparative Primate Biology Neurosciences, vol. 4. Alan R. Liss, Inc., New York, pp. 1–38.

Stephan, H., Baron, G., Frahm, H.D., 1991. Comparative Brain Research in Mammals, vol. 1. Insectivora: With a Stereotaxic Atlas of the Hedgehog Brain. Springer Verlag, New York.

Stephan, H., Bauchot, R., Andy, O.J., 1970. Data on the size of the brain and of various parts in insectivores and primates. In: Noback, C.R., Montagna, W. (Eds.), The Primate Brain. Appleton-Century-Crofts, New York, pp. 289–297.

Stephan, H., Frahm, H.D., Baron, G., 1981. New and revised data on volumes of brain structures in insectivores and primates. Folia Primatol. 35, 1–29.

Sternberger, S.R., 1983. Biomedical image processing. IEEE Comput. Soc. 6, 22–34.

Taylor, A.B., 2002. Masticatory form and function in the African apes. Am. J. Phys. Anthropol. 117, 133–156.

Travers, J.B., Norgren, R., 1983. Afferent projections to the oral motor nuclei in the rat. J. Comp. Neurol. 220, 280–298.

Travers, J.B., Rinaman, L., 2002. Identification of lingual motor control circuits using two strains of pseudorabies virus. Neuroscience 115, 1139–1151.

Turnbull, W.D., 1970. Mammalian masticatory apparatus. Field Mus. Nat. Hist. Fieldana Geol. 18, 149–356.

van Hooff, J.A.R.A.M., 1962. Facial expressions in higher primates. Symp. Zool. Soc. Lond. 8, 97–125.

van Hooff, J.A.R.A.M., 1967. The facial displays of catarrhine monkeys and apes. In: Morris, D. (Ed.), Primate Ethology. Aldine, Chicago, pp. 7–68.

van Lawick-Goodall, J., 1968. A preliminary report on expressive movements and communication in the Gombe Stream chimpanzees. In: Jay, P.C. (Ed.), Primates. Holt, Reinhart and Winston, New York, pp. 313–374.

van Schaik, C.P., Fox, E.A., Sitompul, A.F., 1996. Manufacture and use of tools in wild Sumatran orangutans. Implications for human evolution. Naturewissenschaften 83, 186–188.

Verhaart, W.J.C., 1970. The pyramidal tract in the primates. In: Noback, C.R., Montagna, W. (Eds.), The Primate Brain. Appleton-Century-Crofts, New York, pp. 83–108.

Walberg, F., 1957. Do the motor nuclei of the cranial nerves receive corticofugal fibers? An experimental study in the cat. Brain 80, 597–605.

Walker, P., Murray, P., 1975. An assessment of masticatory efficiency in a series of anthropoid primates with special reference to the Colobinae and Cercopithecinae. In: Tuttle, R.H. (Ed.), Primate Functional Morphology and Evolution. Mouton Publishers, pp. 135–150.

Welt, C., Abbs, J.H., 1990. Musculotopic organization of the facial motor nucleus in *Macaca fascicularis*: a morphometric and retrograde tracing study with cholera toxin B-HRP. J. Comp. Neurol. 291, 621–636.

Wree, A., Schleicher, A., Zilles, K., 1982. Estimation of volume fractions in nervous tissue with an image analyzer. J. Neurosci. Methods 6, 29–43.

Zeller, A.C., 1987. Communication by sight and smell. In: Smuts, B.B., Cheney, D.L., Seyfarth, R.M., Wrangham, R.W., Strusaker, T.T. (Eds.), Primate Societies. University of Chicago Press, Chicago, pp. 433–439.

Zilles, K., Rehkämper, G., 1988. The brain, with special reference to the telencephalon. In: Schwartz, J.H. (Ed.), Orang-utan Biology. Oxford University Press, New York, pp. 157–176.